IEEE Access
Multidisciplinary | Rapid Review | Open Access Journal

Received July 29, 2019, accepted August 9, 2019, date of publication August 21, 2019, date of current version August 30, 2019.

Digital Object Identifier 10.1109/ACCESS.2019.2936471

Improvement of Alternative Non-Raster Scanning Methods for High Speed Atomic Force Microscopy: A Review

SAJAL K. DAS[1], FAISAL R. BADAL[1], MD. ATIKUR RAHMAN[1], MD. ATIKUL ISLAM[1], SUBRATA K. SARKER[1], AND NOROTTOM PAUL[2]

[1]Department of Mechatronics Engineering, Rajshahi University of Engineering & Technology, Rajshahi 6204, Bangladesh
[2]Information and Communication Technology Division, Bangladesh Hi-Tech Park Authority (BHTPA), Dhaka 1207, Bangladesh

Corresponding author: Faisal R. Badal (faisalrahman1312@gmail.com)

This work was supported and funded by Bangabandhu Rajshahi Hi-Tech Park (Borendro Silicon City), Project under Bangladesh Hi-Tech Park Authority, Information and Communication Technology Division.

ABSTRACT The invention of the nanotechnology adds a new branch to investigate and control the physical properties of matters at atomic level. The aim of this technology is to image the characteristics of metals, biological organs, and polymers. Scanning probe microscopy (SPM) opens a new branch to analysis the atomic properties of the matters. Atomic force microscopy (AFM), a branch of SPM, is a versatile tool of nanotechnology to image both conductive and non-conductive matters with high resolution. Commercial AFM uses raster scanning technique to produce image of the matters that is responsible for low scanning speed and image quality. The performances of AFM are hampered due to low bandwidth of the scanning unit and vertical Proportional-Integral (PI) controller and may damage the surface of the samples. Different non-raster scanning techniques such as sinusoidal, rotational, spiral, cycloid, and lissajous scanning have been proposed to overcome the limitations of raster scanning method by providing high scanning speed, image quality, and resolution. This paper presents a survey of raster and non-raster scanning methods for high speed AFM and provides a compression between them in term of scanning speed, bandwidth and highest achievable scanning frequency. The control techniques applied to the AFM for improving raster, sinusoidal, spiral, cycloid, and lissajous scanning methods are studied in this paper to find most optimum scanning technique for AFM.

INDEX TERMS Atomic force microscopy, raster scanning method, sinusoidal scanning method, rotational scanning method, spiral scanning method, cycloid scanning method, Lissajous scanning method, scanning speed, resolution.

I. INTRODUCTION

Nanotechnology is the important invention of the modern science to control the properties of biological organs, metals, and polymers. The behavior of particles largely depends on its surface properties.The surface properties change due to number of reasons such as environmental impact and disturbance. The atomic properties of the particles for the application of biological science are quite challenging to measure by naked eyes [1].

The behavior of a biological sample is mysteries and almost impossible to visualize without the help of instruments. Microscope is an important tool used to visualize the atomic properties of surfaces that magnifies and resolves many properties of particles. Macroscopic image of the objects such as plants and animals can easily be obtained by using microscopes. But, it is unable to provide the details information such as the position and the conditions of different viruses or bacteria presented in the organs or on the surface of the object. The limitations of the microscope are overcome by changing the magnification and resolving abilities. Electron microscope (EM) and atomic force microscope (AFM) have a large magnification and resolving abilities that produce an image of the surface at the molecular level [2].

The Electron microscope captures the image of the surface by using a beam of electron. It releases a beam of electron on the surface that interacts with the atoms of the particles and

The associate editor coordinating the review of this article and approving it for publication was Yingxiang Liu.

produces signal to capture image in a raster pattern [3]. This technique is largely used to capture the image of biological and inorganic specimens to analysis the present situation and structure of the tissues, cells, microorganisms, metals, and crystals. There are two types of electron microscope, i.e. scanning electron microscope (SEM) and transmission electron microscope (TEM).

Transmission electron microscope is generally used to capture the image of thin sample such as tissues and cells [4]. The image is captured by releasing a high voltage electron beam from an electron gun that is controlled by tungsten filament cathode. This electron beam is accelerated by the anode. The electron beam passes through the sample and generates image in atomic level that is observed by the objective lens of TEM. The resolution of the scanned image is poor and it can only produce image of thin sample which is less than 100 nm [5].

Scanning electron microscope is used to capture the image of the sample of a surface by using a beam of electron. This technique follows the principle of raster scanning method to capture an image [6]. A focused electron beam is directed onto the surface across a rectangular area by SEM that interacts with the atoms of the surface. The surface loses energy which is converted to low energy secondary electron. The emission of the secondary electron is collected by detectors and this information is converted into image of the sample of the surface. It provides the details information as compared to TEM. This technique can enhance the properties of the surface and capture image of a large sample. But the resolution of the scanned image by SEM is lower than the TEM. Its application is limited to only solid and inorganic samples [7].

The intrinsic contrast of the surface produced by electron microscope is low. The surface may damage due to the effect of electric beams which limits its application. Again, this technique produces two-dimensional image only. The limitations of the electron microscope are overcome by using scanning probe microscope (SPM) [8]–[10]. It is able to produce atomic image of the biological, chemical, and material surface with high intrinsic contrast. The SPM consists of a sharp probe that takes the reading of a tip and produces image with high resolution [11].

There are several form of SPM such as, scanning tunneling microscope (STM), scanning near-field optical microscope (SNOM), atomic force microscope (AFM) and electrostatic force microscope (EFM). The STM, proposed by G. Binning ang H. Rohrer in 1981, is the scanning process that takes image of conductive materials such as semiconductors and metals [12]. A voltage is applied between the tip of the STM and the surface whose image is be scanned. The voltage difference is responsible to produce tunneling current that acts as the function of the distances between them. The STM technique can scan only conductive materials [13], [14]. Nonconductive materials can not be scanned by this method [15].

Scanning near-field optical microscope is also known as near-field scanning optical microscope is used in nanotechnology [16], [17]. It consists an aperture having smaller diameter than the excitation wavelength. This aperture is used to release an excitation laser light on the surface of the sample and scan the sample at small distance to produce near-field below the aperture. Thus, the resolution of the beam is limited to the diameter of the aperture. Low working distance is the main limitation of SNOM.

Electrostatic force microscope is another kind of SPM that is used to create image of a sample in atomic level. This technique follows the noncontact operation mode between the surface and cantilever [18], [19]. A voltage is applied between the tip of the cantilever and the surface of the sample to measure electrostatic force. The information such as the potential and charges of the surface are recorded to construct image of the sample. Its operation mode is limited to only noncontact mode that is the main limitation of this technique.

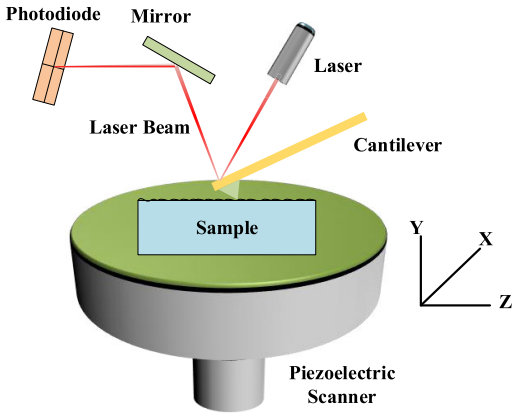

FIGURE 1. Illustration of atomic force microscope.

The limitations of STM, SNOM, and EFM are overcome by the development of atomic force microscope. Atomic force microscope is a scanning probe microscope having high resolution that can scan both conductive and nonconductive materials in fraction of a nanometer [13], [14]. The schematic diagram of AFM is shown in Fig. 1. It conducts three dimensional images by using inter-atomic force between the tip and the surface of the sample. It is more reliable and nondestructive technique as compared to the electron microscope. This technique can even work within liquid that makes it different from others [20]. It plays an important role in the field of biology, polymer science, material science, and pharmaceutical science. In the application of the investigation of virus, proteins, DNA, AFM is largely used [11].

Commercial AFM follows raster pattern to image the matter [21], [22]. The raster pattern is produced by applying triangular wave along x-axis and ramp or staircase signal along y-axis of the positioning units. The triangular wave consists of all odd harmonics of the fundamental frequency that reduces the scanning speed of the AFM to 1% of the resonant frequency of the scanning unit. To improve the scanning speed of the AFM, different scanning methods are

introduced such as sinusoidal [23], rotational [48], spiral [24], cycloid [25], and lissajous scanning method [26]. These techniques overcome the limitations of the raster scanning method. However, the initial scanning speed of the spiral scanning is slow whereas the cycloid scanning method scans an area two times that limit the performance of this scanning method. Different control techniques have been proposed to improve the scanning quality, bandwidth, and resolution of various scanning methods.

Reference [22] presents a survey on raster, sinusoidal raster, spiral, and lissajous scanning for AFM based on the scanning and sampling frequency. A comparison of these scanning method and the design of vertical axis controller are described in [27]. A survey on improving raster scanning for AFM is presented in [28], [29] that describes the nonlinear behaviors of the scanning unit and it's control technique. Reference [30] presents a survey on the behavior and working methods of piezoelectric actuators against different nonlinearities. The relationship between the scanning speed and sampling frequency are listed in [21], [25].

Although techniques of various scanning methods and their operations for the AFM has been reviewed in the aforementioned references, however the summary of the control techniques to improve the scanning accuracy of the non-raster methods of the AFM needs to be addressed. In this paper, we first derive the mathematical expression of the working principle for the raster, sinusoidal, rotational, spiral, cycloid, and lissajous scanning techniques, then we summarize the performances of the scanning methods for a given scanning time and pixels-per-line and the summarization shows that lissajous scanning method performs faster as compared to the other scanning methods. References [28], [29] provides a summarization of the performances between raster, spiral, cycloid, and lissajous methods. However, they did not provide any comparison between these methods. We then, summarize and compare the performances of the control techniques that have been applied for improving non-raster imaging performances of the AFM. The summarization is done to find the achievable accuracy in term of the closed-loop bandwidth, scanning speed, and scanning frequency to find out most optimum scanning technique for AFM.

This paper is organized in the following way: Section II describes the basics of AFM and its components. Different operating mode and scanning method are described in Section III and IV. The performance of open-loop and closed-loop system is investigated in Scetion V and VI. The comparative analysis of raster and non-raster scanning method and future recommendation are evaluated in Section VII and VIII. This paper is concluded in Section IX.

II. ATOMIC FORCE MICROSCOPE'S FEATURES

Atomic force microscope is the technology to scan the surface of objects and magnify it to make it ease to analysis and produce image based on inter-atomic force or van-der-waals force. This technology was proposed by C.F.Quate, Ch.Gerber and G.Binning in 1986 to overcome the limitations of the STM [31]. It consists of a cantilever manufactured by microfabrication technique around 1988 that makes it ease to scan the surface of the sample. The AFM technology becomes largely reliable after inventing optical lever technique that efficiently detects the deflection of cantilever [11]. A laser light is used at the tip of the cantilever that transmits light on the surface of the sample for scanning. The light reflected from the surface is tracked by a photo detector that monitors the deflection of the tip position and produces image based on the tip deflection [11], [18].

At the early age, only contact mode was available [32]. This technique may damage the surface of the sample due to the continuous interaction between the tip and the surface. Tapping mode of the AFM, discovered in 1993, overcomes the problem of contact mode and produces high resolution image. But, the imaging rate at this stage was very slow that could not scan the surface in a proper time frame [32]. In 1994, a high speed scanner was introduced to increase the imaging rate that could scan the surface only x and z direction due to lower bandwidth [32]. This technique was improved in 2001 by using fast electronics and optical deflection detector with small cantilever that was responsible to increase the imaging rate to 12.5 frame/s [20].

Force measurement, imaging, and manipulation is the most three important properties of AFMs. The AFM can measure the force that is introduced between the probe of the tip and the surface of the sample. This force can be used to analysis the mechanical properties of the object such as stiffness, Young's modulus etc. The force imposed by the sample on the probe deflects the position of the tip which is used to make a three-dimensional image [33]. Manipulation is the process to change the properties and characteristics of samples by using force between the probe of the cantilever and the surface. The manipulation is controlled to achieve required shape for the application of the cell simulation, atomic manipulation and others [1], [34], [35]. The most important features of the AFM that makes it a widely used imaging tool are summarized as follows:

(i) It can produce the image of the sample in three-dimension such as x, y and z direction for better observation.

(ii) The resolution of the image is high enough as compared to electron microscope or STM. The atomic resolution in x-y plane becomes 0.1 to 1.0 nm while in the z direction it is 0.001 nm [1], [34].

(iii) Electron microscope can damage the surface of the sample and the accuracy may be reduced due to different artifacts. There is no artifacts in AFM that protects the surface and provides high accuracy.

(iv) This technique can scan and produce image at conditions such as air and liquid and does not need vacuum environment or any surface preparation.

A. COMPONENTS OF AFM

The basic block diagram to operate AFM is shown in Fig. 2. Atomic force microscope consists of several components such as cantilever, tip/probe, laser source, deflection detector,

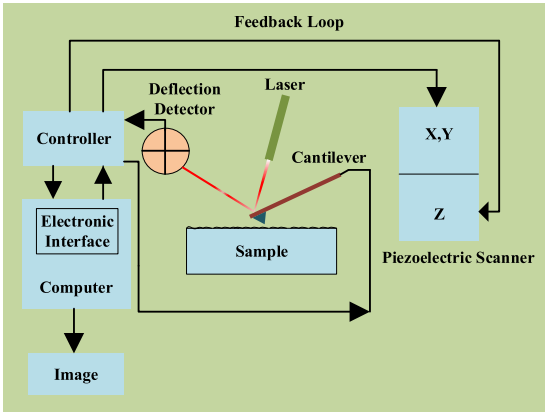

FIGURE 2. Block diagram of atomic force microscope.

feedback loop, and piezoelectric scanner. The size and accuracy of these components is managed in a controlled way to produce high resolution image of the surfaces. This section describes the different components of AFM.

1) CANTILEVER

Cantilever is an important element of the AFM that acts as a force sensor. It works like a spring for force measurement. The shape and size of the cantilever depends on the application. The spring constant (k) of the cantilever is controlled between 0.01-100 nm to achieve small sensitivity to force. The size of the cantilever is minimized for high speed AFM [1], [15]. The cantilever vibrates at resonant frequency (f) that can be represented as

$$f = \frac{0.56t}{l^2}\sqrt{\frac{E}{12\rho}}$$

and the spring constant (k) can be given by

$$k = \frac{wt^3E}{4l^3}$$

where t and w is the cantilever thickness and width, L is the length of the cantilever, E is the Young's modulus and ρ is the density of the cantilever material. Silicon nitride (Si_3N_4) is largely used for soft cantilever whose Young's modulus is 1.461011 N/m^2 and $\rho = 3,087$ kg/m^3. To increase the imaging rate of the AFM, the mass of the cantilever needs to reduce by minimizing the dimension of the cantilever. Thus, the resonant frequency increases [20]. The sensitivity of the cantilever can be represented as:

$$\frac{\Delta\alpha}{\Delta r} = \frac{3}{2l}$$

where $\Delta\alpha$ is the angle change of the cantilever end and Δr is the change of end displacement of the cantilever. Thus, with the decreasing of the cantilever size, the sensitivity of the optical deflection increases. AFM with small cantilever and large ratio of f/k can be used as pulse and frequency modulation AFM. When a cantilever is fabricated with piezoelectric film, it becomes self-actuated and self-sense its deflection [11], [20].

AFM is associated with different kinds of forces such as van-der-waals, double layer, capillary, and adhesive force. The operation of AFM is largely experienced van der waals force. When the distance between the tip and surface is less than r = 100 nm, they experiences van-der-waals force. With the increase of the distance, the interaction force between the tip and cantilever is reduced. At r > 100 nm, there is no force applied on the cantilever as shown in Fig. 3(a). The attractive interaction is produced if r < 100 nm and the cantilever is bent as shown in Fig. 3(b). A very small value of r such as r << 100 nm, bends the cantilever in reversed direction as shown in Fig. 3(c) due to the overlapping of the atom cloud [15].

2) DEFLECTION DETECTOR

The probe of the cantilever contains a laser source to incident laser beam onto the surface of the sample to detect the deflection of the tip. This deflection is focused by using a lens with high numerical aperture. This lens also collects the beam reflected back from the surface at the same time. Polarization splitter and quarter wavelength plate is used to separate and identify the incident and reflected beams. Optical beam deflection detector is largely used to increase the imaging rate of the AFM [11], [15]. The amplitude of the oscillation of cantilever is measured by using different methods where the peak and bottom voltage is captured. The frequency of the deflection signal is calculated by using Fourier method to detect the deflection amplitude of the cantilever. For better performance, the bandwidth of the system must be two times higher than the resonant frequency of the cantilever [11], [15].

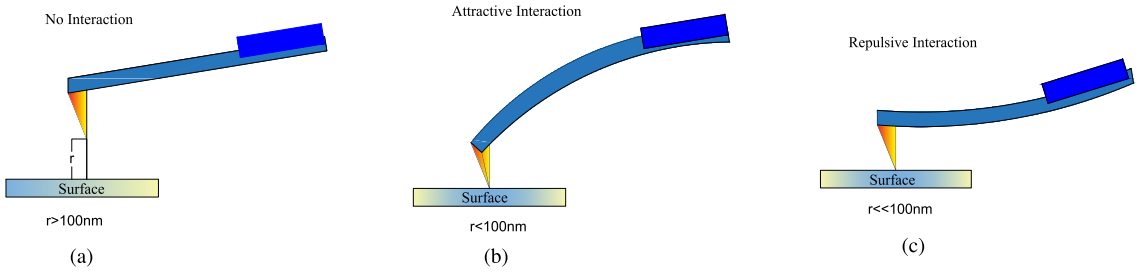

FIGURE 3. Deflection of cantilever at (a) r = 100 nm, (b) r < 100 nm, and (c) r << 100 nm.

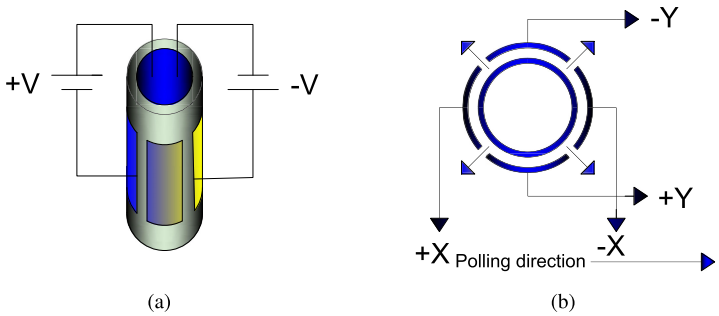

FIGURE 4. (a) Structure of piezoelectric Tube Scanner and (b) Representation of axis of the PTS.

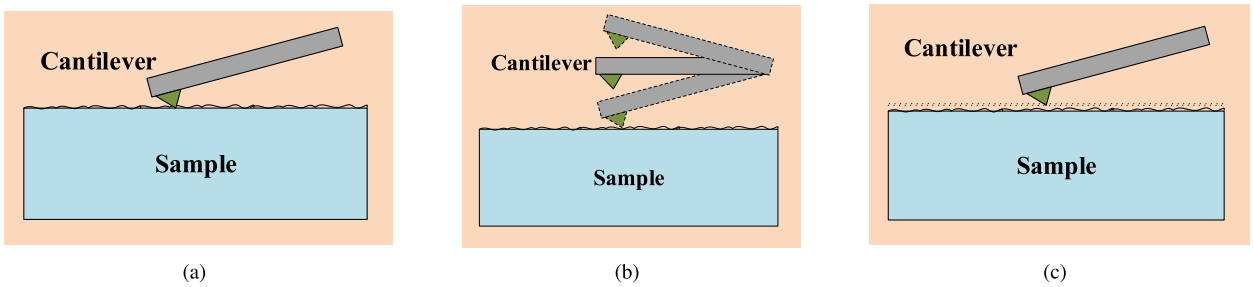

FIGURE 5. Mode of operation (a) Contact mode, (b) Tapping mode, and (c) Non-contact mode.

3) SCANNING UNIT

The scanning unit is used to produce movement between the tip and the surface of the sample as shown in Fig. 4. Unwanted vibration may be produced in the operation of high speed scanning that reduces the accuracy and reliability of the system and damages the surface. This unwanted vibration is reduced by using three method such as, (i) minimize the impulsive force produced by high speed actuator, (ii) increase the resonant frequency of the cantilever, and (iii) reduce the quality factor [11], [15], [20].

Counterbalancing technique is used to minimize the impulsive force in case of high speed actuator [36]. One way to reduce the impulsive force, z-piezoactuator is used which is placed at the four corners of the surfaces. It can move to the counter direction freely that reduces the unwanted mechanical vibration. Thus, it reduces impulsive force produced in the AFM.

A higher resonant frequency is produced by minimizing the size of the cantilever and increasing the ratio of f/k. With the decreasing of the size, the interferences between three axis is increased that is minimized by using a ball-guide stage or blade spring [37], [38].

The quality factor of the cantilever is reduced by using Q-control which is a damping technique. The Q-control is applied to the z-scanner to measure the displacement or the output signal from the electric circuit. This technique increases the bandwidth to almost 150 kHz and reduces the quality factor to almost 0.5 [39].

4) CONTROL LOOP

To control the deflection of the cantilever, a closed-loop feedback is used with AFM. A set point is addressed in the feedback loop that reduces the error between the set point and measured deflection and controls the position of the tip of the cantilever. The deflection force between the tip and surface is very important in case of biological science. An uncontrolled force can damage the biological surface [36]. A dynamic PID controller can resolve this problem which changes the set-point automatically with the situation and properly controls the deflection of the cantilever.

5) ELECTRONICS

AFM consists of computer and data-acquisition system to control the data, produce and display the image. A z-driver is essential to increase the current capacity, slew rate, and bandwidth and reduce the noise and output resistant [20].

III. OPERATION MODES OF AFM

There are three operation modes of the AFM depending on application such as (i) contact mode, (ii) tapping mode, and (iii) non-contact mode. The distance and sensed force is different in different mode.

A. CONTACT MODE

Contact mode of the AFM was introduced first and it is the simplest mode of operation of the AFM is shown in Fig. 5(a). The cantilever is controlled to make a contact between the

tip and the surface of the sample. The distance between the tip and the surface is less than a few Angstroms and the operation takes place in the repulsive region is shown in Fig. 6. The tip makes a permanent soft contact with the surface. The force experienced by the tip is constant such as 10^{-9} that can be determined by using Hooke's law such as $F = -k\Delta x$ [15], [40]. The constant deflection of the cantilever is controlled by feedback loop which keeps that deflection at a set-point continuously.

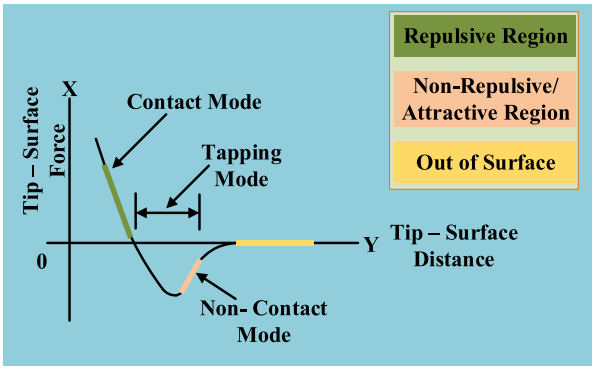

FIGURE 6. Force vs distance curve between tip and surface of the sample.

The spring constant of the cantilever should be kept low for better imaging that can vary between 0.01 to several N/m. This techniques is used to analysis the mechanical property of object by proper modulation of the tip force with an actuator. The capillary force acting on the tip can be reduced by immersing both probe and sample in the liquid. Thus, in liquid, the force is reduced and does not produce any effect in the sample. The surface experienced the force by the tip is the cantilever and capillary force that varies from 10^{-8} to 10^{-6} N.

There are two phases of operation of contact mode such as: (i) constant force and (ii) constant height mode. In constant force mode, the deflection of the cantilever is kept constant by applying a constant force on the tip. When the cantilever deflection and predefined deflection are different, the positioning unit is excited to change the height of the sample with respect to the cantilever. This phase is good for imaging rough surface with high resolution [38]. The constant force may damage the soft sample by changing its local flexure. The resolution may be reduced by the capillary force.

A constant height is always controlled in constant height mode where the deflection of the cantilever is changed. High scanning speed is the main advantage of the this method. The limitation of this method is that the smoothness of the surface must be high. In case of biological surface, the contact mode technique is not reliable due to continuous contact. The biological surface is very soft. If the shear and vertical forces are not controlled properly, it can damage the biological surface easily. Low resolution of the image is the another drawback of this mode of operation [18].

B. TAPPING MODE

Fig. 5(b) represents the tapping mode operation of AFM that overcomes the problems of contact mode. This technique is suitable for soft biological organs. The resolution of the image produced by tapping mode is quite high. The distance between the tip and the surface is intermediate where the cantilever operates at resonant frequency with fixed amplitude. The sensed force by the probe of the cantilever remains attractive region where this amplitude is quite small such as 1 nm. A large amplitude such as 100 nm takes the sensed force to the repulsive region [38], [41].

A amplitude drop is measured during the interaction of the tip and the surface which is controlled at a pre-set level. It can eliminate the shearing force acting on the tip. Tapping mode can be operated in both air and liquid medium [42]. In the air medium, tip is fabricated with a piezoelectric crystal that makes the cantilever to oscillate at or below its resonant frequency. The amplitude of this oscillation is almost 20 nm to 100 nm. The tip touches the surface softly. Different kinds of forces such as van der waals force, electronic force are experienced by the cantilever when the tip touches the surface of the sample. It can also operate in the liquid medium where the interaction force on the tip is reduced. This operation is largely suitable for biological surfaces [43].

This technique efficiently images the soft material with out making any damage and provides linear operating range. when the tip come contact to the sample, any change of the oscillating cantilever amplitude hampers the proper determination of the forces exerted on the tip. The change of resonant frequency is more sensitive which is the another limitation of this mode [44].

C. NON-CONTACT MODE

Non-contact mode is the process where the tip is kept at a constant distance from the sample is shown in Fig. 5(c). The distance between the tip and sample in this case is almost 50-150 angstroms and the tip is experienced attractive van der waals force that is weaker than the repulsive force [18]. The cantilever is fixed with a mechanical device that controls the oscillation at or larger its resonant frequency that can be represented as

$$\omega = \sqrt{\frac{k}{m}}$$

where k is spring constant having value 10-100 N/m and m is mass of the cantilever. The operation mode of non-contact mode are two types such as (i) amplitude modulation where the cantilever is excited by a external signal having constant amplitude and phase, and (ii) frequency modulation where the cantilever is oscillated at resonant frequency. The stiffer cantilever of this mode increases the force sensitivity and decreases bending of the cantilever [45]. The forces experienced by the tip remain at the attractive region whose value is quite low such as 10^{-12} N. Thus, the surface of the sample

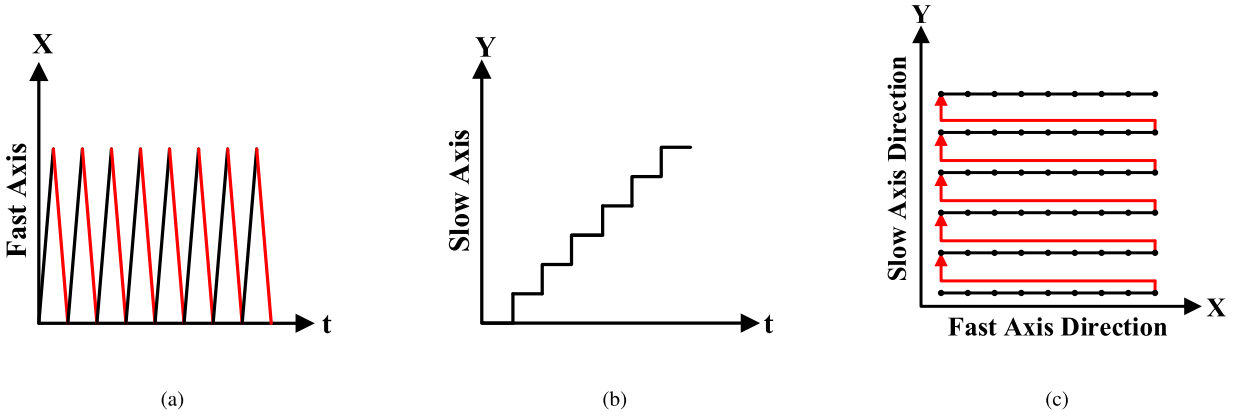

FIGURE 7. (a) Triangular signal applied to fast axis, (b) Staircase signal applied to slow axis, and (c) Raster pattern.

is not damaged by this technique. Poor resolution of the image may be occurred due to the large distance in this mode. The distance can be reduced in ultra-high vacuum (UHV) to increase the resolution of the image [38].

IV. SCANNING METHOD OF AFM

AFM is the technique to scan the surface of an object to analysis. The imaging speed and rate of AFM is slow which makes it time consuming. Thus, the quality of the image at high scanning speed becomes low. Since the physical property of biological surface is not constant, the speed of AFM needs to be faster with high accuracy. The precise positioning of piezoelectric tube scanner (PTS) in x, y, and z axes improves the image quality of the AFM. It consists of two electrode for longitudinal positioning, two electrode for lateral positioning and one electrode for vertical positioning. The speed and accuracy of PTS largely depends on the cross-coupling between its axes, nonlinearities of the materials, resonant dynamic behavior of positioning system. Different scanning method have been proposed to control these limitations and improve the scanning speed of AFM.

A. RASTER SCANNING METHOD

Raster scanning method is largely used for commercial AFM is presented in Fig. 7. Here, the movement of the sample or the probe of the cantilever is controlled by piezoelectric scanner tube in three-direction. In this scanning method triangular waveform is applied at the x axis of the scanner is shown in Fig. 7(a), is also known as fast axis. On the other hand, a ramp or staircase waveform is applied along the y axis which is the slow axis of the scanner is shown in Fig. 7(b) [21], [22]. This technique increases the scanning speed by using a triangular waveform of high frequency.

The rectangular area of the image using raster scanning process can be represented as

$$K = L^2$$

where, L is the length of the scanned image. In raster scanning method, the number of pixel per lines in the image is calculated as,

$$n = \frac{L}{p} + 1$$

where p is the pitch length of the image. The trajectory distance for raster scanning is

$$S = 2L \times n$$

The resolution of the scanned image along x- and y-axis can be represented by

$$R = \frac{L}{n}$$

The scanning frequency and period of the raster are given by

$$T_{ras} = \frac{2(n-1)}{f_{sam}}$$

$$f_{ras} = \frac{1}{T_{ras}}$$

The total required time to scan an image is represented by

$$T_{total} = \frac{n - 0.5}{f_{ras}}$$

where f_{sam} is sampling frequency and f_{ras} is the scanning frequency.

The main problem of using triangular waveform is that it consists of all odd harmonics of the fundamental frequency that hampers the accuracy of the image. The amplitude of the harmonic signal is decreased by $1/n^2$, where n is the number of harmonic. To increase the speed of the AFM, fast triangular waveform is applied. But, it increases the mechanical resonance of AFM and vibration of the scanner that reduces the quality of the image. The scanner speed is kept 10-100 times lower i.e. 1% as compared to the first resonance frequency of the scanner for better performance [22]. The resonance frequency of AFM is normally used as 1 kHz. So, the scanning speed of piezoelectric tube scanner is limited to 10 Hz. A number of nonlinearities are also produced in triangular waveform such as creep, hysteresis etc. that distort the scanning image of the surface of the sample [24], [25].

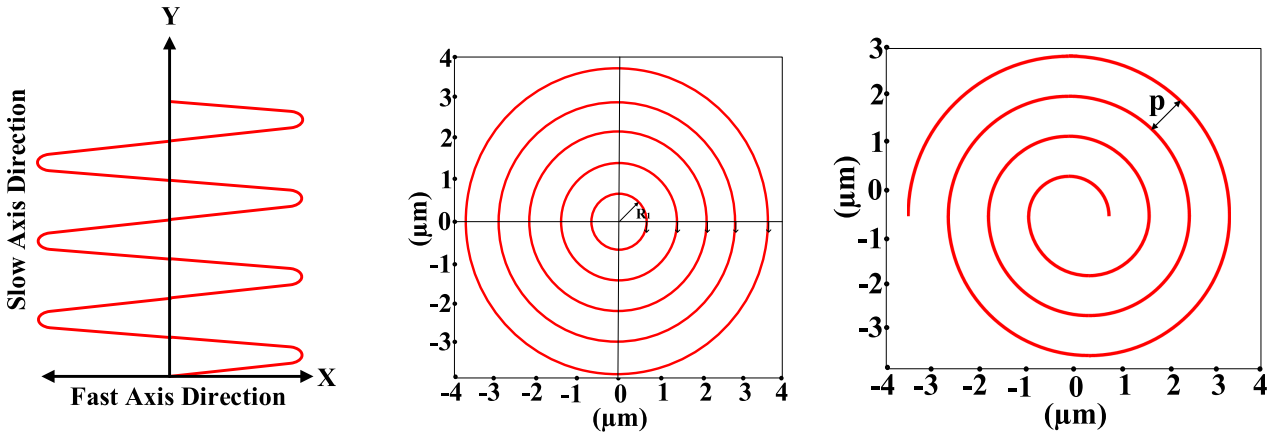

FIGURE 8. (a) Sinusoidal scanning method, (b) Rotational scanning method, and (c) Spiral scanning method.

B. SINUSOIDAL SCANNING METHOD

Sinusoidal scanning is an alternative method of the conventional raster scanning is shown in Fig. 8(a) to scan the sample with high scanning speed. It is an non-raster scanning method based on sinusoidal trajectory. The harmonics due to the triangular signal is minimized here because it uses a sinusoidal trajectory along the x-axis and a ramp signal along the y-axis [23], [46]. The y-axis is used to shift the sample in steps or continuously. The trajectory of raster scanning is specially square wave that is a summation of an infinite number of sinusoidal wave having infinite frequencies that are the responsible of mechanical vibration. On the other side, the sinusoidal scanning consists of only one sine signal with one frequency. As a result, the scanning rate can be increased to the first resonance of the scanning tube. The mathematical representation of sinusoidal scanning method can be represented as [27], [47],

$$x_{sn}(t) = Asin(\omega t)$$
$$y_{sn}(t) = vt$$

If $\omega = 2\pi f_{sn}$, where, f_{sn} is the scanning frequency, then,

$$x_{sn}(t) = Asin(2\pi f_{sn} t)$$
$$y_{sn}(t) = vt$$

where, A is the scanning amplitude and v is the scanning speed. The maximum resolution of scanned image using sinusoidal scanning can be represented as,

$$x_{res} = \frac{x_{size} - x_{size}/n}{2} sin(\frac{2\pi f_{sn}}{f_{sam}})$$

where, x_{size} is the image length along x-axis having pixel number n and f_{sam} is the sampling frequency. The sampling frequency for fixed scanning frequency can be written as,

$$f_{sam} = 2\pi f_{sn}[arcsin(\frac{2}{n-1})]^{-1}$$

The total scanning time to scan the sample using sinusoidal scanning method can be represented as,

$$T_{total} = (\frac{y_{size}}{x_{res}} - 0.5)T_{sn}$$

where, y_{size} is the size of the pixel along y-axis and T_{sn} is the scanning period that can be written as,

$$T_{sn} = \frac{1}{f_{sn}}$$

Thus, the required scanning time is,

$$T_{total} = \frac{n - 0.5}{f_{sn}}$$

where, $n = \frac{y_{size}}{x_{res}}$ is the number of pixel of the scanned image.

For a fixed scanning time, the scanning frequency of sinusoidal scanning method is similar as the raster scanning method.

C. ROTATIONAL SCANNING METHOD

Rotational scanning is another non-raster scanning approach to achieve high scanning speed with large scanning area [48]–[50]. The sudden change of the velocity of the probe are responsible to produce mechanical vibration of the scanner. This scanning method is efficiently able to reduce these mechanical vibrations and increase the scanning area as compared to the raster scanning method. The rotational scanning pattern has the form of spiral or concentric circle by a proper combination of linear and circular motion of the probe. A series of circle are produced with increasing radius from the center of rotation.

Fig. 8(b) represents the construction of rotational scanning pattern having concentric circular shape that is represented in polar coordinate system. The radial coordinate of the rotational scanning method in the form of polar coordinate system can be represented as,

$$r = \sqrt{(x_s + x_0)^2 + (y_s + y_0)^2}$$

And the polar angle,

$$\varphi = atan2(\frac{y_s + y_0}{x_s + x_0})$$

where, x_s and y_s are the position sensor data to detect the position of the sample along the x- and y-axis and *atan*2 is the arctangent function. It is essential to convert the coordinate system from polar to Cartesian system to construct the scanned image from rotational scanning method. The Cartesian representation of this scanning method can be represented as,

$$x_{rot} = rcos(\phi + \phi_0)$$
$$y_{rot} = rsin(\phi + \phi_0)$$

where ϕ_0 and ϕ is the initial and final rotational angle. The rotational angle ϕ can be represented as $\phi = 2\pi f_{rot} t$, where f_{rot} is the scanning frequency and t is the scanned time. Then, the Cartesian coordinate with zero initial condition,

$$x_{rot} = rcos(2\pi f_{rot} t)$$
$$y_{rot} = rsin(2\pi f_{rot} t)$$

The resolution of the scanned image depends on the distance between the adjacent samples Δl and the change of the rotational angle between two adjacent samples $\Delta\phi$ that can be represented as,

$$\Delta l = 2rsin(\frac{\Delta\phi}{2})$$
$$\Delta\phi = 2\pi f_{rot} \Delta t$$

The scanning time required to scan the total rotational pattern is given as,

$$T_{total} = \frac{2\pi r}{p\omega}$$

where p is the pixel of the scanned image that can be represented by,

$$p = \frac{2x_{size}}{n-1}$$

where, n is the number of pixels on the scanned image and x_{size} is the length of the image along x-axis. For a square image,

$$r = \sqrt{(x_{size})^2 + (y_{size})^2} = \sqrt{2}x_{size}$$

Then, the required scanning frequency for rotational scanning can be represented as,

$$f_{rot} = \frac{n-1}{\sqrt{2}T_{total}}$$

The rotational scanning method is responsible to achieve high scanning speed and scanning area with increasing the resolution of the scanned image. But, its scanning area is limited by the travel range of the radial displacement actuator.

D. SPIRAL SCANNING METHOD

Spiral scanning, shown in Fig. 8(c), a non-raster scanning method, is an advanced technique as compared to raster scanning method of AFM. The limitations introduced in raster scanning method are overcome in spiral scanning method. In this method, the spiral signal is produced by using sine and cosine wave that is also known as Archimedean spiral signal. The distance between the interaction of two spiral curve with a line that passes through the origin of the spiral is known as pitch that is constant in this method. This allow the AFM to scan an surface uniformly. The x and y axis of spiral scanning uses sinusoidal signal having identical frequency that makes the trajectory smooth. When the probe of the cantilever moves, transient may occur which is removed in this scanning process. Another advantage of this method is that it processes scanning of the surface without the requirement of specialized hardware [24], [51].

Two types of pattern is used in spiral scanning method depending the tracking process of the trajectory i.e. (i) constant angular velocity (CAV) and (ii) constant linear velocity (CLV) [24]. The formula of generating a CAV is represented as

$$\frac{d\bar{r}}{dt} = \frac{p\omega}{2\pi} \tag{1}$$

where, p is the pitch and ω is the angular velocity of the spiral, r is the instantaneous radius. The pitch p is given by

$$p = \frac{2 \times spiral\ radius}{number\ of\ curves - 1}$$

Number of curve is equal to the number how much the spiral curve cross the x axis where $y = 0$. Equation (1) can be represented as

$$\int d\bar{r} = \frac{p\omega}{2\pi} \int dt$$

After solving this equation for $r = 0$ when $t = 0$,

$$\bar{r} = \frac{p\omega t}{2\pi} \tag{2}$$

The time required to scan the surface of a sample can be calculated by using the equation,

$$\int_{\bar{r}_1}^{\bar{r}_2} d\bar{r} = \frac{p\omega}{2\pi} \int_{t_1}^{t_2} dt$$

where, $\bar{r}_1$ and $\bar{r}_2$ are the first and last spiral radius and t_1 and t_2 are the initial and final scanning time. If $\bar{r}_1 = 0$ when $t_1 = 0$ and $t_T = t_2 - t_1$, then, the above equation can be represented as

$$t_T = T_{total} = \frac{2\pi\bar{r}_2}{p\omega} \tag{3}$$

where $\bar{r}_2$ can be represented as

$$\bar{r}_2 = \sqrt{{X_{size}}^2 + {Y_{size}}^2}$$

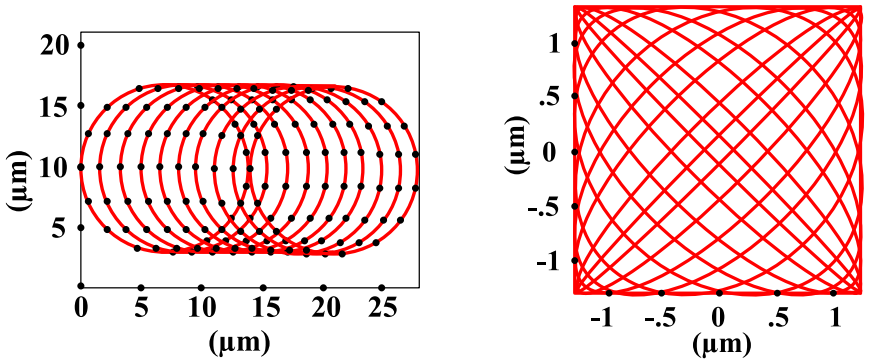

(a) (b)

FIGURE 9. (a) Cycloid scanning method and (b) Lissajous scanning method.

Equation (2) is represented as Cartesian coordinates so that the piezoelectric tube scanner can track the spiral trajectory in the following way,

$$x_a = \bar{r}cos\theta$$
$$y_a = \bar{r}sin\theta$$

where, x_a and y_a is the input of the piezoelectric tube scanner along x and y axis and $\theta = \omega t$, is the angle. The phase errors produced in the scanner signal can be removed by

$$X_a = \bar{r}cos(\theta + \alpha)$$
$$Y_a = \bar{r}sin(\theta + \beta)$$

The frequency response of closed-loop system is used to determine the phase constants α and β. The amplitude varying of this sinusoidal signal is quite slow that able to track a high frequency CAV signal which increases the velocity of the AFM. When The velocity between the tip and the surface of the sample is linear, this technique can not be applied due to its variable linear velocity which is the main limitation of CAV [24].

The limitation of CAV can be overcome by using CLV where $\bar{r}$ and ω is changed continuously to keep the linear velocity constant [24]. The formation of spiral for CLV can be represented as

$$\frac{d\bar{r}}{dt} = \frac{p\bar{v}}{2\pi\bar{r}} \tag{4}$$

where, $\bar{v}$ is the linear velocity of the spiral of CLV. The radius $\bar{r}$ can be calculated from (4) as,

$$\int \bar{r}d\bar{r} = \frac{p\bar{v}}{2\pi}\int dt$$

After solving this equation for $r = 0$ when $t = 0$,

$$\bar{r} = \sqrt{\frac{p\bar{v}t}{\pi}} \tag{5}$$

The angular velocity for the spiral can be represented as

$$\omega = \frac{\bar{v}}{\bar{r}}$$

Putting the value of ω in (5),

$$\omega = \sqrt{\frac{\pi\bar{v}}{pt}}$$

The scanning time of the surface of the sample for CLV can be represented as

$$T_{total} = \frac{\pi\bar{r}_2^2}{p\bar{v}}$$

To track the spiral trajectory, Equation (5) is represented as cartesian coordinates such as

$$x_l = \bar{r}cos\sqrt{\frac{4\pi\bar{v}t}{p}}$$
$$y_l = \bar{r}sin\sqrt{\frac{4\pi\bar{v}t}{p}}$$

The main advantages of spiral scanning is to increase the imaging time and image quality by reducing mechanical resonance. But, the distortion of the image increases with the increasing of the frequency of the system which is the major limitation of spiral mode. CLV technique is more demanding as compared to CAV during the design of controller of AFM. The main limitations of CAV is that its scanning frequency is constant and linear velocity is not constant all time that reduces the quality of the scanning image. These are overcome by CLV that increases the scanning speed and provides uniform resolution of the image. But, initially it is suffered by high angular frequency [24], [25], [52].

E. CYCLOID SCANNING METHOD

Different technique have been applied to speed up the imaging rate with high scanning area of the surface of the sample. Fig. 9(a) represents cycloid method that is another non-raster scanning method which increases the scanning speed of AFM. This method overcomes the problems of raster scanning and spiral scanning methods. The cyclic pattern is produced using sine and cosine signal. The lateral axis is

used to track the sine wave and the other axis tracks the cosine wave. It is important to keep the frequency of both signal equal with a slow ramp. The scanning technique can produce high quality image at high scanning speed without the need of any special tools or the damping mode of the scanner [25]. The horizontal distance between the scan lines are always fixed and the center of the scan area is scanned twice. The pattern of the cycloid is increased during scanning operation that makes it useful to the analysis of string and the feature of the sample. This scanning technique scans only the desired area of the sample instead of the whole area and thus, it reduces the scan time [25], [53]. The trajectory of the cycloid pattern can be produced using the lateral axes of nanopositioner as follows,

$$x_c = \alpha t + \bar{r} sin\omega t$$
$$y_c = \bar{r} cos\omega t$$

If the scanning frequency of AFM is f_{cy}, then, $\omega = 2\pi f_{cy}$, and the equation can be represented as

$$x_c = \alpha t + \bar{r} sin\ 2\pi f_{cy} t$$
$$y_c = \bar{r} cos 2\pi f_{cy} t$$

where, α is the rate of the ramp signal, r is the magnitude of the input signal x. The pitch p of the cycloid pattern is fixed that represents the largest pixel at constant frequency and can be represented as

$$\alpha = \frac{p\omega}{2\pi} = \frac{p}{T}$$

where, T is the period of the sine wave. The distance between the samples are kept fixed during uniform scanning that produces an image having $p \times p$ pixels. The pixels can be represented as

$$p = \frac{4\bar{r}}{2n-1}$$

where, n is pixel number along the y axis. The x axis has $2n$ lines. The total scanning time can be represented by

$$T_{total} = \frac{n+1}{f_{cy}}$$

The sampling point of the cycloid pattern is tracked to produce AFM image where the pitch for both cycloid and raster image is kept same. The vector length between the cycloid and raster point can be given as

$$D = \sqrt{(A_x - B_x)^2 + (A_y - B_y)^2}$$

To improve the image quality of the surface, the vector length should be less than $p/2$ such as

$$D < \frac{p}{2}$$

and the sampling frequency f_{sm} must be kept larger than the scanning frequency f_{cy} as below

$$f_{sm} \geq 4nf_{cy}$$

The cycloid method provides high quality image as compared to the raster, sinusoidal or spiral scanning method and it does not excite the resonance of the piezoelectric scanner of the AFM.

F. LISSAJOUS SCANNING METHOD

Lissajous is an another non-raster scanning method to increase the imaging rate of AFM at high speed is shown is Fig. 9(b). This scanning method tracks a purely sinusoidal signal having fixed amplitude but different phase and frequency. The frequency spectrum of sinusoidal signal is narrow. It is easy to track a sinusoidal signal for the nanopositioner whose bandwidth is limited as compared to triangular of ramp signal [21], [54]. The scanning area is divided in a number of small grids that increases the resolution of the image. This technique is useful is the research application of nano-material and biological surface [26]. The scanner of AFM are forced to track the following signal to produce lissajous pattern,

$$x_L = A_x cos(\omega_x)t$$
$$y_L = A_y cos(\omega_y)t$$

If $\omega = 2\pi f_{liss}$ where, f_{liss} is the scanning frequency, then the equation can be arranged as

$$x_L = A_x cos(2\pi f_x)t$$
$$y_L = A_y cos(2\pi f_y)t$$

where, A_x and f_x represent the amplitude and frequency of sinusoidal signal of x-axis and A_y and f_y represents the amplitude and frequency of sinusoidal signal y-axis. The difference between frequencies f_x and f_y is used to determine the shape of the lissajous pattern. The phase difference between the sinusoidal signal can be generated by producing a variety of lissajous pattern [55]. The time period of lissajous pattern can be calculated by using the difference of frequencies along x and y axis as follows,

$$T_L = \frac{1}{|f_x - f_y|}$$

The lissajous pattern is converted from a line to a circle in first quadrant and returned to its line shape in the next quadrant. The frequency ratio along the x and y axis can be represented as

$$\frac{f_x}{f_y} = \frac{2i}{2i-1}$$

where, n is an integer. The value of $2i$ and $2i-1$ are coprime, then

$$f_x = 2if_{liss}$$

and

$$f_y = (2i-1)f_{liss}$$

where, f is the fundamental frequency of the pattern such as $f = f_x - f_y$. The whole trajectory can be produce within the

TABLE 1. Compression of scanning frequency for different scanning method.

Scanning Method	Total Scanning Time	Required Scanning Frequency Formula	Scanning Frequency (Hz)	Comparison of Scanning Frequency
Raster Scanning	$T_{total} = \frac{n-0.5}{f_{ras}}$	$f_{ras} = \frac{n-0.5}{T_{total}}$	511.5	f_{ras}
Sinusoidal Scanning	$T_{total} = \frac{n-0.5}{f_{sn}}$	$f_{sn} = \frac{n-0.5}{T_{total}}$	511.5	f_{ras}
Rotational Scanning	$T_{total} = \frac{n-1}{\sqrt{2}f_{rot}}$	$f_{rot} = \frac{n-1}{\sqrt{2}T_{total}}$	361.332	$0.66f_{ras}$
Spiral Scanning	$T_{total} = \frac{2\pi r_2}{p\omega}$	$f_{spi} = \frac{n}{\sqrt{2}T_{total}}$	362.03	$0.707f_{ras}$
Cycloid Scanning	$T_{total} = \frac{n+1}{f_{cy}}$	$f_{cy} = \frac{n+1}{T_{total}}$	513	$1.003\ f_{ras}$
Lissajous Scanning	$T_{total} = \frac{\pi n}{2\sqrt{2}f_{liss}}$	$f_{liss} = \frac{\pi n}{2\sqrt{2}T_{total}}$	568.40	$1.1\ f_{ras}$

time period $t\epsilon[0, \frac{T_L}{4}]$. The lissajous pattern cuts itself in many point within a defined region. The time interval between two crossing point can be represented by

$$T_{in} = \frac{1}{4i(2i-1)f}$$

The value of i must be kept large to increase the crossing point as compared to the point touching the edge. The resolution of lissajous pattern is defined as

$$R_{liss} = \frac{\pi A_x A_y}{i\sqrt{{A_x}^2 {A_x}^2}}$$

where i can be represented as

$$i = \frac{\pi A_x A_y}{R_{liss}\sqrt{{A_x}^2 {A_x}^2}} = \frac{n\pi}{2\sqrt{2}}$$

The total imaging time of lissajous scanning can be represented as

$$T_{total} = \frac{i}{f_{liss}} = \frac{n\pi}{2\sqrt{2}f_{liss}}$$

Lissajous scanning method is reliably applied where high precision is required such as biological sample. This technique efficiently increases the scanning speed and accuracy with resolution. Sometimes, the corner information is lost which is the main limitation of this scanning technique.

The required scanning frequency for different scanning method is listed in Table 1 for total scanning time 1s and 512 pixels-per-line. Table 1 represents that the lissajous scanning method is 1.1% and cycloid scanning method is 1.003% faster as compared to raster and sinusoidal scanning method. On the other hand, spiral scanning method is 0.707% and rotational scanning method is 0.66% slower as compared to raster and sinusoidal method. Table 2 represents the compression of different scanning method.

V. OPEN-LOOP PERFORMANCE

High speed atomic force microscope is largely demanded with high precession and resolution of the scanning image. The open-loop response of AFM is free from any external noise due to the absence of additional sensor and special hardware. Digital signal processor, displacement sensor are required to implement the dynamics of the piezoelectric tube scanner. In case of open-loop, the dynamics of the scanner must be accurate for better performance. With the change of load, the resonance frequency of the scanner is changed that changes the model dynamics of the scanner and hampers the AFM performance. Thus, the scanning speed is limited to 1% of the resonant frequency of the scanner. Again, the area can not be scanned uniformly due to the presence of hysteresis that provides inaccurate tracking of the reference signal and produces wrong conclusion [69].

VI. CONTROLLER DESIGN

To eliminate the problems of open-loop technique, closed-loop technique is implemented with AFM. The closed-loop technique consists of sensors and controllers for precious tracking of the reference signal. The error between the input and output is sensed by the sensor and fed to the controller to minimize this by applying proper control signal. It is important to require a controller design to achieve high bandwidth, phase and gain margin, reduce the impacts of nonlinearity and uncertainties and track the reference efficiently to increase the scanning rate of AFM. Fig. 10 represents a list of proposed controller for different scanning method.

A. CONTROL METHODS APPLIED FOR RASTER SCANNING TECHNIQUE

The odd harmonics of the triangular wave reduces the resolution of raster scanning. The harmonics excite the resonance of the piezoelectric tube scanner and produce a distorted signal at piezoelectric scanner that hampers the scanning image with distorted surface topology. This distorted image is responsible to make a wrong conclusion [2]. To control and increase the efficiency of raster scanning several control technique have been proposed is shown in Table 3.

A lag-lead controller for raster scanning has be presented [66]. It reduces the steady state error by controlling the transient response of the system. The impact of the first resonance of the scanner can not be eliminated by this control technique that produces some attenuation of the signal.

To control the raster scanning, a feedback controller has been proposed [29], [66], [83]–[85]. This control technique

TABLE 2. Highlights of different scanning methods.

Parameters	Raster	Sinusoidal	Spiral	Cycloid	Lissajous	Rotational
Wave signal	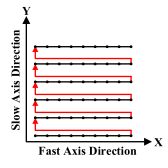	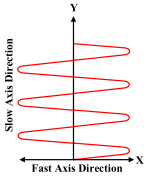	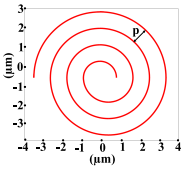	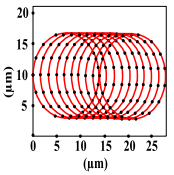	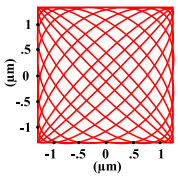	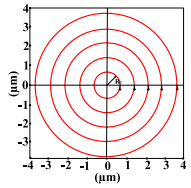
Scanned Image	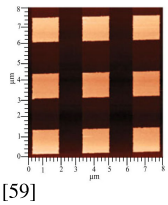 [59]	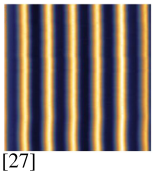 [27]	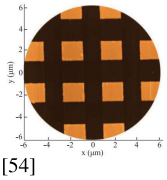 [54]	 [56]	 [57]	 [51]
Generation of Waveform	Triangular signal is applied along x-axis (fast axis) and ramp or staircase signal is applied along y-axis (slow axis)	Sine wave is applied along x-axis and ramp signal is applied along y-axis	Sine wave is applied along x-axis and cosine wave is applied along y-axis with same frequency	Sine wave is applied along x-axis and cosine wave is applied along y-axis with same frequency with a ramp signal	The interference of sinusoidal signals having single tone, constant amplitude and frequency applied in two-dimensional space produces lissajous wave	Sine wave is applied along the x-axis and combine the linear and circular motion of the probe
Representation	$X_r = \int sgn(sin(x))dx$ $Y_r = y; y \geq 0$	$X_{sn} = Asin(2\pi f_{sn}t)$ $Y_{sn} = vt$	$X_s = \bar{r}cos(2\pi f_{spi})t$ $Y_s = \bar{r}sin(2\pi f_{spi})t$	$X_c = \alpha t + \bar{r}sin(2\pi f_{cy})t$ $Y_c = \bar{r}cos(2\pi f_{cy})t$	$X_l = A_x cos(2\pi f_x)t$ $Y_l = A_y cos(2\pi f_y)t$	$X_{rot} = rcos(2\pi f_{rot})t$ $Y_{rot} = rsin(2\pi f_{rot})t$
Advantages	(i) Easy to operate, (ii) Easy to implement, (iii) Preferable for slow operation	(i) Easy to apply, (ii) Minimize the harmonics, (iii) Minimize the mechanical vibration	(i) No mechanical resonance, (ii) Surface is scanned uniformly, (iii) High quality of scanned image, (iv) Limited frequency spectrum	(i) Required no specialized hardware arrangement, (ii) More preferable with high uniform scanning speed, (iii) Able to scan video-rate properly	(i) Low tracking error, (ii) Faster scanning speed, (iii) Do not excite the piezoelectric scanner resonance, (iv) Construct multi-resolution image	(i) Minimize the mechanical vibration, (ii) Increase the scanning area
Limitations	(i) High mechanical resonance, (ii) Vibration of the scanner, (iii) Low image quality, (iv) Scanning speed is much lower as compared to piezoelectric scanner resonance	(i) Low scanning frequency, (ii) Constant velocity is not possible	(i) High distortion of the image at high spiral frequency, (ii) Linear velocity of CAV is not constant, (iii) CAV is not preferable when the motion between tip and surface needs to be linear, (iv) High angular frequency of CLV initially	(i) Corner information may be lost, (ii) Same area is scanned twice	(i) Difficult to construct, (ii) Difficult to implement and operate	(i) Scanning area may be hampered due to the limited travel range of the radial displacement actuator, (ii) Constant velocity is not possible
Application	(i) Image capture, (ii) Printing, (iii) Computer graphics, (iv) Video timing, (v) Fire control radar, (vi) Sound scanner [37], [60]	(i) Barcode reader, (ii) Laser scanner, (iii) Image forming, (iv) Pattern forming, (v) DNA sequencing, (vi) Quality inspection, (vii) Air bearing, (viii) Galvanometer mirror [61]	(i) Scroll compressor, (ii) Gas compression, (iii) Identification of human tremor, (iv) Digital light processing, (v) Image capture [62]–[64]	(i) Roller coaster, (ii) Worm gear, (iii) Wankel rotary engine, (iv) Cycloidal reducer, (v) Image capture [65], [66]	(i) Vibration Study, (ii) Audio reactive graphics, (iii) Analysis of analog signal, (iv) Frequency measurement of tuning fork, (v) Measurement of oxygen saturation, (vi) Detection of phase difference, (vii) Image capture, (viii) Pattern recognition [67], [68]	(i) Image forming, (ii) Pattern forming, (iii) DNA sequencing, (iv) Light processing, (v) Gas compression [52], [53]
Proposed Year	1990 [69]	2000 [70]	2004 [71]	2010 [56]	2012 [57]	2015 [52]

consists of inductive and optical sensors and custom-made capacitive that ensures to reduction of the mechanical vibration and creep. The calibration is made automatically and data lost is reduced in this control technique by using rectangular scanning. PID, PI or integral controller are the feedback controller having high feedback gain to reduce the scanner

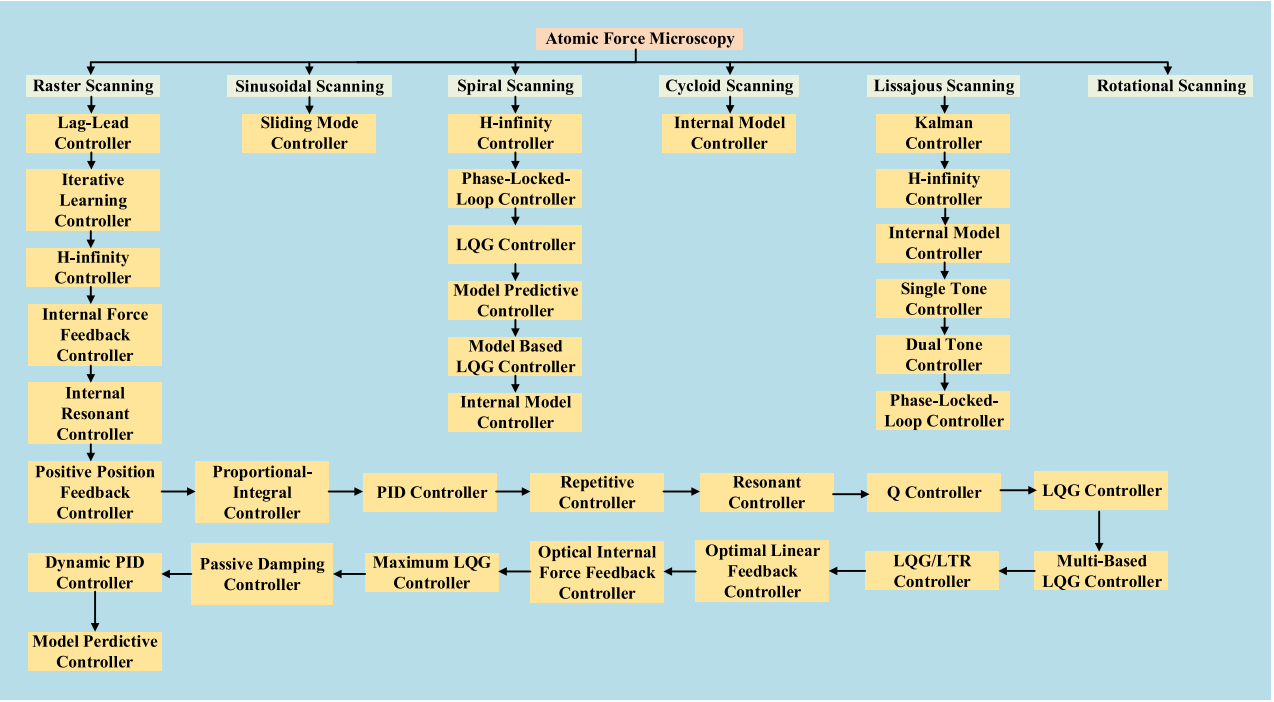

FIGURE 10. Proposed controllers for different scanning methods of atomic force microscope.

vibration [38], [56], [86]–[88]. The performance of this control technique is hampered due to the presence of hysteresis and uncertainties. The gain margin and closed-loop bandwidth of these controller is limited that requires an additional notch filter.

To overcome the positioning error between the tip and surface at high scanning speed and the unwanted modification, a feedforward controller has been presented [29], [83]. The input shaping approach of this controller reduces the vibration of the piezoelectric tube scanner and minimizes the scan time by reducing the input energy. This control approach provides a high closed-loop bandwidth at high scanning speed. It overcomes the limitation of feedback controller by controlling hysteresis using inverse compensation technique. Sensitivity of the parameters, complexity of the model and poor robustness at the presence of uncertainties are the main limitations of this control approach. Iterative learning controller (ILC) is a feedforward controller having high bandwidth [73]. The design criteria of ILC is difficult as the iteration number is very high to converge.

The limitation of feedforward control approach is overcome by the integration of a feedback controller with feedforward controller. The modeling and tracking error can not be reduced by only feedforward controller. A feedback controller is integrated with it to reduce the error due to the presence of uncertainties and improve the tracking performance [29], [83], [89], [90]. The combination of both controller ensures high closed-loop bandwidth and robustness by shaping the reference signals.

H-infinite controller has been efficiently designed to speed up the AFM [66], [70], [91], [92]. This control technique is designed based on by minimizing the l_2 gain of the input that controls the output of the system. This controller largely depends on the system order. Thus, an H-infinite controller for high order system is difficult to design which requires the knowledge of digital signal processing and hampers the design of the unmodeled plant.

The integral force feedback (IFF) and optimal integral force feedback (OIFF) have been proposed to track the reference signal and damp the first resonance of the scanner [71], [79]. These controllers are limited to the closed-loop pole placement. Positive velocity and position feedback (PVPF) control approach overcomes the limitation of IFF and OIFF [93]. It improves the tracking error by rejecting the unwanted noise and enhances the pole placement of the system.

To damp the resonant frequency of the scanner, integral resonant controller (IRC) has been proposed [72], [94]. It is a first order control approach, applied to the scanner directly, that are able to damp out multiple resonant modes. This control approach is only responsible to control the vibration of the scanner. The tracking error can not be controlled by this controller. To increase the closed-loop bandwidth and reduce the steady-state error to zero, an integral controller is mounted with this controller in feedforward mode. The integral action controls the phase margin and feedforward approach increases the bandwidth of the system. A multivariable IRC controller has been proposed [95] with resonant

TABLE 3. Highlights of different controller for raster scanning of AFM.

Name of the controller	Year	Closed-loop Bandwidth (Hz)	Achievable Highest Scanning Frequency (Hz)	Advantages	Limitations
H-infinity Controller [73]	2005	1000	125	(i) Damp out the higher resonance of the scanner	(i) Difficult to construct high order controller, (ii) Require the knowledge of DSP, (iii) Low pass filter is required
Integral Force Feedback Controller [74]	2008	2070	100	(i) High tracking performance, (ii) Damp out the high resonance of the scanner	(i) Poor pole placement capability
Integral Resonant Controller [75]	2008	490	31	(i) Reduce the mechanical vibration, (ii) Damp out the first resonance of the Scanner, (iii) High bandwidth	(i) Poor tracking capability, (ii) External integral controller is required
Iterative Learning Controller [76]	2009	400	100	(i) High closed-loop bandwidth	(i) Require large number is iteration.
Positive Position Feedback Controller [77]	2009	350	60	(i) High closed-loop bandwidth	(i) Low gain- and phase-margin
PD Controller [40]	2010	400	450	(i) Ease to design, (ii) Ease to implementation, (iii) Low order transfer function	(i) Low bandwidth, (ii) Low gain- and phase-margin
Repetitive Controller [78]	2011	420	100	(i) Reduce the steady-state error, (ii) No data lost	(i) Poor performance due to harmonics, (ii) External filter is required
Resonant Controller [79]	2012	400	62.5	(i) High bandwidth	(i) Add unwanted frequency to the system
Model-Based LQG Controller [80]	2013	850	125	(i) Produce linear motion between the tip and the surface, (ii) High closed-loop gain and bandwidth	(i) Add noise due to external sensor
LQG/LTR Controller [81]	2014	630	300	(i) High tracking capability, (ii) High robustness	(i) Poor performance due to dynamic model
Optimal Integral Force Feedback Controller [82]	2014	310	100	(i) High tracking performance, (ii) Damp out the high resonance of the scanner	(i) Poor pole placement capability
Maximum LQG Controller [72]	2014	450	200	(i) High robustness, (ii) High closed-loop gain	(i) Poor tracking capability
Velocity Feedback Controller [83]	2014	450	100	(i) High closed-loop gain and phase margin, (ii) High tracing performance	(i) Incorrect data from actuator or sensor make a system not to be a passive system
Dynamic PID Controller [84]	2015	2000	450	(i) Ease to design, (ii) Ease to implementation, (iii) Low order transfer function	(i) Poor Performance due to change of temperature, (ii) Low bandwidth and closed-loop gain
Model Predictive Controller [85]	2015	450	125	(i) High gain and phase margin, (ii) High robustness, (iii) Low noise	(i) Low bandwidth, (ii) Poor performance due to cross-coupling

controller to compensate the mechanical vibration at resonant frequency.

The resonant controller and positive position feedback (PPF) controller have been proposed having tracking performance [74], [76], [87], [88]. They damp the resonant mode of the piezoelectric scanner. These controllers are designed based on negative imaginary (NI) approach. A system $G(s)$ is called NI if it follows the following condition $j[G(j\omega) - \bar{G}(j\omega)] \geq 0$. For a NI system, the real part of the eigenvalues of $j[G(j\omega) - \bar{G}(j\omega)]$ is always equal or greater than to zero for all $\omega\epsilon(0, \infty)$. Lower gain and phase margin is the main limitation of PPF controller. The resonant controller, on the other hand, adds unwanted frequency to the system. To overcome these problems passive damping controller has been designed based on the combination of mixed passivity, NI and small gain approach. This control approach have high gain and phase margin and damps the first resonant of the scanner. This control approach may increase the noise of the external sensor.

References [75] and [96] present a repetitive controller has been proposed to control the Z-axis movement and speed of the scanner by controlling bandwidth and the quality of the image. This also controls the interaction force between the tip and surface. It consists of a memory loop that generates the repetitive input signals and matches the period of the signals to reduce the steady-state error and track the reference signal. To reduce the harmonics introduced in the signal, a filter is mounted with this controller.

The optimal scan speed has been regulated by controlling the quality factor of the cantilever of AFM. Active Q control has been propose to regulate this Q factor [97]. The time delay of the displacement of cantilever is measured by velocity feedback that estimates the Q factor. The unmodeled dynamics may introduce unwanted resonance of the scanner that needs an extra resonant controller to damp these resonance.

Another damping technique to control the positioning of tip and surface is linear-quadratic Gaussian (LQG) controller. It reduces the unwanted vibrations of the scanner and controls the interaction force. But, alone a LQG controller can not minimize the vibration properly and exhibits poor robustness. To overcome this problem a loop transfer recovery (LTR) is combined with LQG controller [78]. This control loop

TABLE 4. Highlights of different controller for sinusoidal scanning of AFM.

Name of the controller	Year	Closed-loop Bandwidth (Hz)	Achievable Highest Scanning Frequency (Hz)	Advantages	Limitations
Sliding Mode Controller [50]	2013	750	125	(i) High robustness, (ii) Eliminate the effect of disturbance	(i) Scanning path is not smooth and optimized

obtains the linear-quadratic regulator (LQR) properties by using Kalman filter or feedback controller. The LQG/LTR approach able to minimize the scanner vibration at high frequency in the presence of hysteresis.

The effect of nonlinear behavior of piezoelectric tube scanner is controlled by model-based LQG controller [77]. The presence of nonlinearity distorts the scan trajectory and position tracking. The controller is designed with vibration compensator to damp out the vibration and produce linear motion between tip and sample.

To reduce the interaction force between the tip and sample, optimal linear feedback controller (OLFC) with state-dependent riccati equation (SDRC) has been proposed [101], [102]. This control technique finds the linear control application of a nonlinear system and increases the stability of the system. It takes the system to a desirable periodic orbit from a chaotic state. SDRC finds the optimal solution of static equation and takes the system to periodic state using feedback control.

Maximum LQG controller, a special form of LQG, efficiently damps the resonant of the piezoelectric scanner [69]. This control algorithm has been designed by using H_2 norm which solves two riccati equations. This control approach finds the optimal input by solving LQG performance index. It provides robust performance against unmodeled dynamics and uncertainties.

The design of velocity feedback controller, a passive damping controller, is used to damp of the high resonance of the scanner [80], [103]. The system having transfer function $G(s)$ is called passive if $\mathrm{Re}[G(j\omega)] \geq 0$ for all $\omega > (0, \infty)$. The bandpass nature of this controller provides high gain and phase margin. The incorrect data of the actuator and sensor are the main limitation to make a system not to be passive.

The uncontrolled bending cantilever may damage the surface of the sample. A dynamic PID controller is presented to control the feedback gain in order to control the bending of the cantilever and the speed of the AFM [81], [104]. The controller is designed based on Fourier transformation of cantilever oscillation signals. The performance of this control technique is limited due to the increase of temperature and the presence of liquid that changes the oscillation efficiency of the cantilever.

To damp the resonant of the piezoelectric scanner, increase the bandwidth, Model predictive controller (MPC) has been proposed [82]. A vibration compensator is integrated with MPC to damp out the unwanted vibration of the scanner. The estimated future trajectory is used to minimize the cost function of MPC. This control approach efficiently tracks the reference signal and increases the scanner speed. The effect cross-coupling reduces the performance of this controller.

B. CONTROL METHODS APPLIED FOR SINUSOIDAL SCANNING TECHNIQUE

In sinusoidal scanning, a sine wave is applied along the x-axis instead of triangular signal to reduce the harmonics. Still the scanning speed and resolution control is important for high speed AFM. Sliding mode controller has been proposed to enhance the speed and precision of AFM [47] is described in Table 4. This controller has been designed based on internal model principle with neural network. This control algorithm is efficiently control the parameters uncertainties and nonlinear effects.

C. CONTROL METHODS APPLIED FOR SPIRAL SCANNING TECHNIQUE

Around 1976, the spiral scanning method is introduced to overcome the problems of raster scanning and speed up the scanning process of AFM in medical sector. The main limitation of this method is that, the distribution of the sampling points are difficult to uniform in 2D plane. Again, constant linear velocity is another challenge of this method [2]. The proposed controller is listed in Table 5.

To increase the speed of AFM, the trajectory of spiral path has been modified [21], [105]. Archimedean spiral is one having constant loop distance. It is suitable for both CAV and CLV that uses almost all data of the sample to produce image. The optimal spiral is made by combining the benefits of CAV and CLV that regulates the angular frequency and velocity to enhance high speed of AFM.

The design of H-infinite controller has been presented to increase the speed and tracking capability of AFM [98]. The controller is designed with sliding peak filter for better performance to track the reference signal in the feedback loop. To control the motion of both axis, two H-infinite controller is applied in each axis. The feedback loop is mounted with sliding peak filter that shifts the scanner frequency efficiently. The combined control algorithm provides high bandwidth and better performance as compared to single H-infinite controller.

The Phase error between two sinusoidal signals along x- and y-axis is controlled by model-based optimal LQG controller. But, at same frequency the performance of this control approach is limited with some phase error. A phase-locked-loop controller has been proposed to minimize this error and increase the scanning resolution of AFM [52]. This controller is designed based on PI controller. The phase

TABLE 5. Highlights of different controller for spiral scanning of AFM.

Name of the controller	Year	Closed-loop Bandwidth (Hz)	Achievable Highest Scanning Frequency (Hz)	Advantages	Limitations
H-infinity Controller [103]	2011	1000	100	(i) Reduce the vibration of the scanner, (ii) High Bandwidth	(i) Poor tracking capability, (ii) Poor robustness
Phase-Locked-loop Controller [55]	2014	450	120	(i) Reduce the phase error	(i) PI controller is required
LQG Controller [104]	2014	500	125	(i) High tracking performance, (ii) Large gain- and phase-margin and bandwidth	(i) Low robustness at uncertainties, (ii) Butter-worth filter is required
Model Predictive Controller [24]	2015	540	180	(i) High closed-loop gain, (ii) High robustness	(i) Difficult to construct, (ii) Low bandwidth
Model-Based LQG Controller [2]	2016	700	125	(i) High closed-loop gain and bandwidth	(i) Add noise due to external sensor, (ii) Low tracing performance, (iii) Vibration compensator is required
Internal Model Controller [105]	2017	3000	150	(i) Reduce the nonlinearity of the system	(i) External integrator is required

TABLE 6. Highlights of different controller for cycloid scanning of AFM.

Name of the controller	Year	Closed-loop Bandwidth (Hz)	Achievable Highest Scanning Frequency (Hz)	Advantages	Limitations
Internal Model Controller [32]	2018	6000	1600	(i) Low bandwidth does not affect the performance	(i) Low tracing performance due to the error along x-axis

error measured by phase detector is controlled by PI control approach. The resolution and scanning speed of this method is high as compare to raster scanning.

The phase error between the input and output signal is regulated by LQG controller [99]. This control approach is designed with an integrator to eliminate the tracking error and a reference signal model is incorporated in the system model. The change of the frequency of the spiral is slower with time that makes the scanner to track the signal efficiently and increase the scanning rate. The robustness of this controller is hampered by uncertainties and unwanted noise that requires a butter-worth filter to filter the noise.

The design of a model-based linear quadratic Gaussian (LQG) controller has been proposed to speed up the scanning rate of AFM [2]. A slowly varying sine and cosine signal are applied along x- and y-axis to uniformly cover the scanning area. The resultant Archimedean spirals has low frequency that properly tracks the reference signal and always remains in steady-state. This controller is applied along x- and y-axis to reduce the steady-state error and track the spiral signal efficiently that increases the closed-loop bandwidth of the system which is equal the first resonant frequency of piezoelectric scanner.

An internal model controller (IMC) has been proposed to reduce the tracking errors which is produced due to the increase of sinusoidal frequency [55], [100]. This controller is designed based on internal model principle that can be applied for the spiral scanning with varying amplitude of the reference signal that regulates the reference signal and uncertainties within the feedback control loop. The nonlinearity is reduced by applying an integrator and imaginary pole at resonant frequency.

The Model predictive control approach has been proposed to reduce the nonlinear behavior and increase the scanning rate of AFM [111]. The controller is designed by integrating a integral action and Kalman filter to reduce the steady-state error. It can predict the future state of the system. To increase the damping ratio, feedback controller has been proposed [24]. The high damping ratio of this control algorithm increases the closed-loop gain and bandwidth by rejecting the first resonance of the scanner. This control technique consists of two loop. One loop consists of positive position feedback controller that increase the damping ratio and the other contains integral for better tracking of the reference.

D. CONTROL METHODS APPLIED FOR CYCLOID SCANNING TECHNIQUE

The cycloid scanning method is applied for high scanning rate and resolution of AFM. But, at same frequency and scanning area, its scanning rate is lower as compared to spiral scanning. This is due to the presence of an extra ramp signal along the X-axis and the data points are overlapped [2].

Internal model controller has been proposed to improve the scanning speed of AFM [25] is shown in Table 6. This control approach is designed with an integral controller along the X-axis to reject the disturbance of low frequency. This control structure can efficiently track the reference signal. The bandwidth does not effect the tracking performance of this control approach. The tracking performance is affected by the error along the X-axis.

E. CONTROL METHODS APPLIED FOR LISSAJOUS SCANNING TECHNIQUE

The proposed controller to improve the performance of lissajous scanning method is listed in Table 7. Internal model controller (IMC) has been proposed to increase the scanning speed of AFM [106]. The lateral axis of the scanner is forced

TABLE 7. Highlights of different controller for lissajous scanning of AFM.

Name of the controller	Year	Closed-loop Bandwidth (Hz)	Achievable Highest Scanning Frequency (Hz)	Advantages	Limitations
Internal Model Controller [111]	2012	15000	600	(i) High Bandwidth, (ii) Track constant, ramp, sinusoidal signal	(i) Poor tracking capability, (ii) External integrator is required (iii) Re-designing is required in many case
Single Tone Controller [112]	2015	600	125	(i) Does not excite the resonance frequency of the scanner,(ii) Regulate the shape of the reference signal	(i) Low tracing performance, (ii) High periodic error
Dual Tone Controller [113]	2016	730	152	(i) Reduce the periodic error, (ii) Reduce the impact of disturbance	(i) Poor performance due to uncertainty
Phase-Locked-loop Controller [114]	2017	1050	150	(i) Reduce the phase error, (ii) Does not depend on the system modelling	(i) External disturbances is not reduced properly (ii) Eternal feedforward controller is required
Kalman Filter [115]	2017	4600	5000	(i) Does not require re-configuration, (ii) Does not require expert knowledge	(i) Extra vibration controller is required, (ii) Poor tracking performance

to track a purely sinusoidal signal having fixed frequency and amplitude. The scanner is assumed as a parallel-kinematic device whose frequency is high as compared to the resonance frequency. IMC can efficiently tracks the ramp, sinusoidal, and constant signal. This controller has high closed-loop bandwidth and gain. To improve the tracking performance, an external integrator is required. Re-configuration, expert knowledge are required for this controller [106]. A Kalman filter control approach has been proposed to overcome these problems [110]. The controller is designed based on base-band PI controller. This control structure does not require re-configuration. An external vibration controller is required to control the mechanical vibration.

The lissajous scanning method can scan a square area where the spiral and cycloid method can scan round and capsule-shaped area. References [107], [112], and [113] represent a modified model of lissajous scanning by using single-tone and multi-frequency signals to increase the scanning rate of AFM. The tribo-electrification process of this method uses silicon dioxide surface for analysis. This control method can speed up the scanning rate without increasing the resonant frequency of the scanner.

The design of dual tone wave controller has been proposed for high speed AFM application [108] that reduces the periodic error. The single tone controller regulates the shape of the reference signal and the movement of the scanner. But, at driving frequency unwanted motion between the tip and sample hampers the performance of AFM and produces a tracking error. Dual tone controller overcomes the problems of single tone controller by minimizing the effects of the disturbance of each axis. The controller is designed by minimizing H-norm and the parameters is tuned by H-infinite control approach. The presence of uncertainties reduce the efficiency of this control method.

Phase-locked-loop controller has been proposed to track the periodic signal of AFM [109], [114]. The phase error is minimized by regulating and synchronizing the frequency and phase of the input and output signal. It consists of a voltage controlled oscillator, low pass filter, and a phase detector. The limitations of single and double tone controller is overcome by this control approach. A precise model of the system is not important in this case. The external disturbances are not reduced by this control approach that required an external feedforward controller.

VII. COMPARATIVE ANALYSIS BETWEEN RASTER AND NON-RASTER SCANNING TECHNIQUE

Raster scanning method is the first scanning technique developed to scan the surface of the sample that is largely used method for AFM. Although, in many applications such as, image formatting, pattern recognition, computer graphics, scanner, data compression etc., non-raster scanning can be used [49], [58], [59], [62], [64], but raster scanning is largely used method in these applications due to the ease construction of the raster pattern, ease to control, and implementation. As an earlier scanning method, a lot of work has been done on raster scanning which makes it a largely used scanning method. From the innovation of raster scanning, different control algorithm has been developed to improve its performance. But, now-a-days, different non-raster scanning method such as sinusoidal, rotational, spiral, cycloid, and lissajous methods are also largely used in the industrial applications which give better performance as compared to raster scanning. Researchers are now give their concern to develop different control algorithm to improve the performances such as scanning speed, scanning time, scanning area, and resolution of non-raster scanning methods. These non-raster scanning methods give satisfactory result that increases their application in different industrial sector at present. A compression between the contribution of this research work and the existing research work is listed in Table 8.

Commercial AFM uses raster scanning method to produce image of a matter whose scanning speed is limited to 1% of the resonant frequency of AFM. The scanning unit with 1000 Hz resonance frequency is able to produce almost 10 Hz scanning speed for raster scanning method. High mechanical noise and vibration of the scanner limits the image quality of this method. The mechanical noise and vibration of the scanner is overcome by using sinusoidal scanning, rotational scanning, and spiral scanning that improve the image

TABLE 8. Comparison of the contribution between this research work and existing survey paper.

Reference	Highlights	Limitations
Ref. [22]	Summarize the relationship between scanning frequency and scanning time for raster, sinusoidal raster, spiral and lissajous scanning technique	Doesn't discuss the operating mode and control techniques for improving raster and non-raster scanning method
Ref. [27]	Summarize the relationship between scanning frequency and scanning time for raster, sinusoidal raster, spiral and lissajous scanning technique and vertical controller	Doesn't discuss the operating mode and control techniques for improving raster and non-raster scanning method
Ref. [28]	Discuss the effect of nonlinearities and the control method to overcome these effects	Doesn't discuss the control techniques for improving raster and non-raster scanning method
Ref. [31]	Summarize the relationship between the CLV and CAV and compare the performance of different scanning method of AFM	Doesn't discuss the relationship and control method of different scanning method
Present Research	(i) Summarize the basic components, operations and raster and non-raster scanning methods of AFM, (ii) Compares the function and scanning speed between raster and non-raster scanning technique, (iii) Summarize the control technique applied to the AFM for improving raster, sinusoidal, spiral, cycloid and lissajous scanning method based on their bandwidth, scanned frequency, advantages and limitations (iv) Discuss the future improvement required for high speed AFM	-

quality, resolution and bandwidth. But, the scanning speed of sinusoidal scanning is equal to the raster scanning. on the other side, spiral and rotational scanning speed is limited to 0.707% and 0.66% as compared to raster scanning method. The cycloid scanning method is 1.003% faster than raster scanning method. But it's performance is limited because it lost corner information and scans the same area for two times. The limitations of those scanning method are overcome by lissajous scanning method that reduces the mechanical noise, vibration and tracking error by not exciting the scanner. The scanning speed of this method is 1.1% faster as compared to raster scanning method that is largely used for high speed AFM. The ability to construct multi-resolution image and faster speed makes it optimum scanning method for AFM.

VIII. FUTURE RECOMMENDATIONS

The AFM technology has become more demanding in the application of nanotechnology to characterized the biological surface, mechanical elements etc. To increase the scanning speed of AFM, different control techniques have been proposed. Different scanning methods overcome the problems of raster scanning. High scanning speed, resolution, and image quality largely depends on the modelling of the system, measurement units, control systems etc.

Proper system modelling is essential to achieve desired performance of a system. The performance of high speed AFM is largely affected by the unmodelled dynamics. The effects of different nonlinearities such as hysteresis, cross coupling reduces the speed and quality of the imgae. Vertical dynamics, cantilever beam dynamics, and interaction force dynamics need to be accounted in the control technique to overcome these problems. The position sensors add different noise that reduces the scanning speed and resolution of AFM whose model should be considered in the control system. Scanning speed can be increased to decrease the cantilever size. Multiple cantilever can be used at the same time to increase the speed of AFM.

The control technique need to be improved to increase the bandwidth of the system. Different control techniques are interested to control the lateral axis while the vertical axis is controlled by built-in proportional-integral controller that results low bandwidth of AFM. Z-axis controller should be designed to achieve high bandwidth and scanning speed. Two controller can be implemented at the same time whose one controller reduces the nonlinear effect, vibration and the other tracks the signal at high speed.

Control technique should be improved to increase the initial speed of spiral scanning method. The scanning area and speed may be improved by designing different controller for rotational scanning method along the z-axis which will be the future scope for the researchers. Again, cycloid scanning method scans the sample twice that can be overcome. The construction of lissajous pattern is quite complex and largely effected by nonlinearities. A new research area will be introduced to overcome these limitations. The measurement units of AFM such as different sensor should be controlled properly to increase the image quality and bandwidth.

IX. CONCLUSION

This paper presents the summary of the non-raster scanning methods applied to the AFM for fast image scanning at high scanning speeds. Commercial AFM usually uses raster scanning method to investigate the sample of the surface due to ease construction of the raster pattern, ease to control the scanning process, ease to collect the information from the sample, and low operating cost. But the scanning speed of raster scanning is limited to 1% of the resonant frequency of the scanner. A relationship between the scanning speed, scanning time, scanning area, and pixels is investigated in this paper that provides a clear view of the performance of each scanning method. Different control techniques have been summarized in this paper to overcome the problems of raster and non-raster scanning method to increase its imaging rate. Although, the raster scanning is easy to control, but the non-raster scanning methods are able to construct image having

high resolution with high scanning speed. The closed-loop bandwidth and scanning area of non-raster scanning method is high enough as compared to the raster scanning method. A compression between non-raster scanning method such as sinusoidal, rotational, spiral, cycloid, and lissajous and raster scanning method has been listed in Table 1 and 2 to find most optimum scanning method for AFM. Table 1 and 2 ensure that lissajous scanning method provides high scanning speed and high quality of images. Lissajous scanning method is 1.1% faster as compared to raster scanning method and able to construct multi-resolution image without the effect of the resonant of the scanning unit that makes it optimum scanning technique as compared to other scanning technique.

REFERENCES

[1] S. Chatterjee, S. S. Gadad, and T. K. Kundu, "Atomic force microscopy," *Resonance*, vol. 15, no. 7, pp. 622–642, 2010.
[2] H. Habibullah, H. R. Pota, and I. R. Petersen, "High-speed spiral imaging technique for an atomic force microscope using a linear quadratic Gaussian controller," *Rev. Sci. Instrum.*, vol. 85, no. 3, 2014, Art. no. 033706.
[3] A. F. Tryon and B. Lugardon, *Spores of the Pteridophyta: Surface, Wall Structure, and Diversity Based on Electron Microscope Studies*. Springer, 2012.
[4] L. Reimer, *Transmission Electron Microscopy: Physics of Image Formation and Microanalysis*, vol. 36. Springer, 2013.
[5] I. Griffiths, D. Cherns, X. Wang, H.-H. Wehman, M. Mandl, M. Strassburg, and A. Waag, "Characterisation of 3D-GaN/InGaN core-shell nanostructures by transmission electron microscopy," *Phys. Status Solidi C*, vol. 11, nos. 3–4, pp. 425–427, 2014.
[6] L. Reimer, *Scanning Electron Microscopy: Physics of Image Formation and Microanalysis*, vol. 45. Springer, 2013.
[7] P. W. Trimby, "Orientation mapping of nanostructured materials using transmission Kikuchi diffraction in the scanning electron microscope," *Ultramicroscopy*, vol. 120, pp. 16–24, Sep. 2012.
[8] H. Dai, J. H. Hafner, A. G. Rinzler, D. T. Colbert, and R. E. Smalley, "Nanotubes as nanoprobes in scanning probe microscopy," *Nature*, vol. 384, no. 6605, p. 147, 1996.
[9] R. Wiesendanger and W. Roland, *Scanning Probe Microscopy and Spectroscopy: Methods and Applications*. Cambridge, U.K.: Cambridge Univ. Press, 1994.
[10] M. Alexe and A. Gruverman, *Nanoscale Characterisation of Ferroelectric Materials: Scanning Probe Microscopy Approach*. Springer, 2013.
[11] R. N. Jagtap and A. H. Ambre, "Overview literature on atomic force microscopy (AFM): Basics and its important applications for polymer characterization," *Indian J. Eng. Mater. Sci.*, vol. 13, pp. 368–384, Aug. 2006.
[12] J. Tersoff and D. R. Hamann, "Theory of the scanning tunneling microscope," in *Phys. Rev. B, Condens. Matter*, vol. 31, no. 2, p. 805, 1985.
[13] J. Tersoff and D. R. Hamann, "Theory and application for the scanning tunneling microscope," *Phys. Rev. Lett.*, vol. 50, no. 25, p. 1998, 1983.
[14] G. Binnig, H. Rohrer, C. Gerber, and E. Weibel, "Surface studies by scanning tunneling microscopy," *Phys. Rev. Lett.*, vol. 49, no. 1, p. 57, 1982.
[15] B. Kyeyune, "Atomic force microscopy," Ph.D. dissertation, Afr. Inst. Math. Sci., Cape Town, South Africa, 2017.
[16] J. Tisler, T. Oeckinghaus, R. J. Stohr, R. Kolesov, R. Reuter, F. Reinhard, and J. Wrachtrup, "Single defect center scanning near-field optical microscopy on graphene," *Nano Lett.*, vol. 13, no. 7, pp. 3152–3156, 2013.
[17] J.-S. Bouillard, S. Vilain, W. Dickson, and A. V. Zayats, "Hyperspectral imaging with scanning near-field optical microscopy: Applications in plasmonics," *Opt. Express*, vol. 18, no. 16, pp. 16513–16519, 2010.
[18] S. Morita, F. J. Giessibl, E. Meyer, and R. Wiesendanger, *Noncontact Atomic Force Microscopy*, vol. 3. Springer, 2015.
[19] C. Riedel, R. Sweeney, N. E. Israeloff, R. Arinero, G. A. Schwartz, A. Alegría, P. Tordjeman, and J. Colmenero, "Imaging dielectric relaxation in nanostructured polymers by frequency modulation electrostatic force microscopy," *Appl. Phys. Lett.*, vol. 96, no. 21, 2010, Art. no. 213110.
[20] T. Ando, T. Uchihashi, N. Kodera, D. Yamamoto, M. Taniguchi, A. Miyagi, and H. Yamashita, "High-speed atomic force microscopy for observing dynamic biomolecular processes," *J. Mol. Recognit.*, vol. 20, no. 6, pp. 448–458, 2007.
[21] D. Ziegler, T. R. Meyer, A. Amrein, A. L. Bertozzi, and P. D. Ashby, "Ideal scan path for high-speed atomic force microscopy," *IEEE/ASME Trans. Mechatronics*, vol. 22, no. 1, pp. 381–391, Feb. 2017.
[22] Y. R. Teo, Y. K. Yong, and A. J. Fleming, "A review of scanning methods and control implications for scanning probe microscopy," in *Proc. Amer. Control Conf. (ACC)*, Jul. 2016, pp. 7377–7383.
[23] A. J. Fleming, B. J. Kenton, and K. K. Leang, "Bridging the gap between conventional and video-speed scanning probe microscopes," *Ultramicroscopy*, vol. 110, no. 9, pp. 1205–1214, 2010.
[24] I. A. Mahmood, S. O. R. Moheimani, and B. Bhikkaji, "A new scanning method for fast atomic force microscopy," *IEEE Trans. Nanotechnol.*, vol. 10, no. 2, pp. 203–216, Mar. 2011.
[25] N. Nikooienejad, A. Alipour, M. Maroufi, and S. O. R. Moheimani, "Sequential cycloid scanning for time-resolved atomic force microscopy," in *Proc. IEEE/ASME Int. Conf. Adv. Intell. Mechatronics (AIM)*, Jul. 2018, pp. 125–130.
[26] J.-W. Wu, Y.-T. Lin, Y.-T. Lo, W.-C. Liu, and L.-C. Fu, "Lissajous hierarchical local scanning to increase the speed of atomic force microscopy," *IEEE Trans. Nanotechnol.*, vol. 14, no. 5, pp. 810–819, Jun. 2015.
[27] Y. R. Teo, Y. Yong, and A. J. Fleming, "A comparison of scanning methods and the vertical control implications for scanning probe microscopy," *Asian J. Control*, vol. 20, no. 4, pp. 1352–1366, 2016.
[28] M. Rana, H. R. Pota, and I. R. Petersen, "Improvement in the imaging performance of atomic force microscopy: A survey," *IEEE Trans. Autom. Sci. Eng.*, vol. 14, no. 2, pp. 1265–1285, Apr. 2017.
[29] S. Devasia, E. Eleftheriou, and S. O. R. Moheimani, "A survey of control issues in nanopositioning," *IEEE Trans. Control Syst. Technol.*, vol. 15, no. 5, pp. 802–823, Sep. 2007.
[30] J. Peng and X. Chen, "A survey of modeling and control of piezoelectric actuators," *Mod. Mech. Eng.*, vol. 3, no. 1, p. 1, 2013.
[31] G. Meyer and N. M. Amer, "Novel optical approach to atomic force microscopy," *Appl. Phys. Lett.*, vol. 53, no. 12, pp. 1045–1047, 1988.
[32] C. A. J. Putman, K. O. van der Werf, B. G. De Grooth, N. F. van Hulst, and J. Greve, "Tapping mode atomic force microscopy in liquid," *Appl. Phys. Lett.*, vol. 64, no. 18, pp. 2454–2456, 1994.
[33] F. J. Giessibl, "Advances in atomic force microscopy," *Rev. Mod. Phys.*, vol. 75, no. 3, p. 949, Jul. 2003.
[34] H. J. Butt, B. Cappella, and M. Kappl, "Force measurements with the atomic force microscope: Technique, interpretation and applications," *Surf. Sci. Rep.*, vol. 59, nos. 1–6, pp. 1–152, 2005.
[35] P. K. Hansma, V. B. Elings, O. Marti, and C. E. Bracker, "Scanning tunneling microscopy and atomic force microscopy: Application to biology and technology," *Science*, vol. 242, pp. 209–216, Oct. 1988.
[36] D. M. Copolovici and C. Sîrghie, "Structural investigation by atomic force microscopy," *Sci. Bull. ESCORENA*, vol. 8, pp. 23–29, Nov. 2013.
[37] G. Schitter and A. Stemmer, "Identification and open-loop tracking control of a piezoelectric tube scanner for high-speed scanning-probe microscopy," *IEEE Trans. Control Syst. Technol.*, vol. 12, no. 3, pp. 449–454, May 2004.
[38] S. K. Das, H. R. Pota, and I. R. Petersen, "Intelligent tracking control system for fast image scanning of atomic force microscopes," in *Chaos Modeling and Control Systems Design*. Springer, 2015, pp. 351–391.
[39] T. R. Rodrıguez and R. García, "Theory of Q control in atomic force microscopy," *Appl. Phys. Lett.*, vol. 82, no. 26, pp. 4821–4823, 2003.
[40] G. Haugstad, *Atomic Force Microscopy: Understanding Basic Modes and Advanced Applications*. Hoboken, NJ, USA: Wiley, 2012.
[41] R. Proksch and D. G. Yablon, "Loss tangent imaging: Theory and simulations of repulsive-mode tapping atomic force microscopy," *Appl. Phys. Lett.*, vol. 100, no. 7, 2012, Art. no. 073106.
[42] P. K. Hansma, J. P. Cleveland, M. Radmacher, D. A. Walters, P. E. Hillner, M. Bezanilla, M. Fritz, D. Vie, H. G. Hansma, C. B. Prater, J. Massie, L. Fukunaga, J. Gurley, and V. Elings, "Tapping mode atomic force microscopy in liquids," *Appl. Phys. Lett.*, vol. 64, no. 13, pp. 1738–1740, 1994.
[43] L. Zitzler, S. Herminghaus, and F. Mugele, "Capillary forces in tapping mode atomic force microscopy," *Phys. Rev. B, Condens. Matter*, vol. 66, no. 15, 2002, Art. no. 155436.
[44] T. Sulchek, G. G. Yaralioglu, C. F. Quate, and S. C. Minne, "Characterization and optimization of scan speed for tapping-mode atomic force microscopy," *Rev. Sci. Instrum.*, vol. 73, no. 8, pp. 2928–2936, 2002.

[45] C. Sánchez-Sánchez, T. Dienel, O. Deniz, P. Ruffieux, R. Berger, X. Feng, K. Müllen, and R. Fasel, "Purely armchair or partially chiral: Noncontact atomic force microscopy characterization of dibromo-bianthryl-based graphene nanoribbons grown on Cu(111)," *ACS Nano*, vol. 10, no. 8, pp. 8006–8011, 2016.

[46] G. M. Clayton and S. Devasia, "Image-based compensation of dynamic effects in scanning tunnelling microscopes," *Nanotechnology*, vol. 16, no. 6, p. 809, 2005.

[47] C.-L. Chen, J. Wei, Y.-T. Lin, Y.-T. Lo, and L.-C. Fu, "Sinusoidal trajectory for atomic force microscopy precision local scanning with auxiliary optical microscopy," in *Proc. 52nd IEEE Conf. Decis. Control*, Dec. 2013, pp. 348–353.

[48] A. Ulčinas and Š. Vaitekonis, "Rotational scanning atomic force microscopy," *Nanotechnology*, vol. 28, no. 10, 2017, Art. no. 10LT02.

[49] X. Du, N. Kojimoto, and B. W. Anthony, "Concentric circular trajectory sampling for super-resolution and image mosaicing," *J. Opt. Soc. Amer. A, Opt. Image Sci.*, vol. 32, no. 2, pp. 293–304, 2015.

[50] X. Du and B. Anthony, "Concentric circle scanning system for large-area and high-precision imaging," *Opt. Express*, vol. 23, no. 15, pp. 20014–20029, 2015.

[51] M. Rana, H. Pota, and I. Petersen, "Performance of sinusoidal scanning with MPC in AFM imaging," *IEEE/ASME Trans. Mechatronics*, vol. 20, no. 1, pp. 73–83, Feb. 2015.

[52] H. Habibullah, H. Pota, and I. Petersen, "Phase-locked loop-based proportional integral control for spiral scanning in an atomic force microscope," *IFAC Proc. Volumes*, vol. 47, no. 3, pp. 6563–6568, 2014.

[53] Y. K. Yong, S. O. R. Moheimani, and I. R. Petersen, "High-speed cycloid-scan atomic force microscopy," *Nanotechnology*, vol. 21, no. 36, 2010, Art. no. 365503.

[54] A. Bazaei, Y. K. Yong, and S. O. R. Moheimani, "High-speed Lissajous-scan atomic force microscopy: Scan pattern planning and control design issues," *Rev. Sci. Instrum.*, vol. 83, no. 6, 2012, Art. no. 063701.

[55] Y. K. Yong, A. Bazaei, and S. O. R. Moheimani, "Video-rate Lissajous-scan atomic force microscopy," *IEEE Trans. Nanotechnol.*, vol. 13, no. 1, pp. 85–93, Jan. 2014.

[56] S. K. Das, H. R. Pota, and I. R. Petersen, "Multi-variable resonant controller for fast atomic force microscopy," in *Proc. IEEE 2nd Austral. Control Conf.*, Nov. 2012, pp. 448–453.

[57] J. S. Bianco, "Bar code scanner having a light source/photodetector movable in a raster pattern," U.S. Patents 5 175 420, Dec. 29, 1992.

[58] T. Hayakawa, T. Watanabe, T. Senoo, and M. Ishikawa, "Gain-compensation methodology for a sinusoidal scan of a galvanometer mirror in proportional-integral-differential control using pre-emphasis techniques," *J. Vis. Exp.*, vol. 122, Apr. 2017, Art. no. 55431.

[59] D. A. Bluemke and E. K. Fishman, "Spiral CT of the liver," *Amer. J. Roentgenol.*, vol. 60, no. 4, pp. 787–792, 1993.

[60] G. Wang, Y. Ye, and H. Yu, "Approximate and exact cone-beam reconstruction with standard and non-standard spiral scanning," *Phys. Med. Biol.*, vol. 52, no. 6, p. R1, 2007.

[61] H. E. Cline and T. R. Anthony, "Magnetic resonance imaging with interleaved fibonacci spiral scanning," U.S. Patent 6 281 681, Aug. 28, 2001.

[62] A. G. Bodine, "Cycloidal drill bit," U.S. Patents, 4 527 637, Jul. 9, 1985.

[63] X.-G. Ge, J. Li, and L.-P. Wang, and H.-L. Yu, "Application of cycloid in machining polygon parts," *Mach. Tool Hydraulics*, to be published.

[64] D. Karacor, S. Nazlibilek, M. H. Sazli, and E. S. Akarsu, "Discrete lissajous figures and applications," *IEEE Trans. Instrum. Meas.*, vol. 63, no. 12, pp. 2963–2972, Dec. 2014.

[65] K. Ohtsuka, E. Saitoh, H. Kagaya, N. Itoh, S. Tanabe, F. Matsuda, H. Tanikawa, J. Yamada, T. Aoki, and Y. Kanada, "Application of Lissajous overview picture in treadmill gait analysis," *Jpn. J. Comprehensive Rehabil. Sci.*, vol. 6, pp. 33–42, 2015.

[66] N. Tamer and M. Dahleh, "Feedback control of piezoelectric tube scanners," in *Proc. 33rd IEEE Conf. Decis. Control*, vol. 2, Dec. 1994, pp. 1826–1831.

[67] O. Sasaki, T. Kuwahara, R. Hara, and T. Suzuki, "Sinusoidal wavelength-scanning interferometric reflectometry," *Appl. Opt.*, vol. 39, no. 22, pp. 3847–3853, year. 2000.

[68] K. K. Leang, "Iterative learning control of hysteresis in piezo-based nano-positioners: Theory and application in atomic force microscopes," Ph.D. dissertation, Univ. Washington, Seattle, WA, USA, 2004.

[69] S. K. Das, O. U. Rehman, H. R. Pota, and I. R. Petersen, "Minimax LQG Controller Design for Nanopositioners," in *Proc. Eur. Control Conf. (ECC)*, Jun. 2014, pp. 1933–1938.

[70] A. J. Fleming, "Nanopositioning system with force feedback for high-performance tracking and vibration control," *IEEE/ASME Trans. Mechatronics*, vol. 15, no. 3, pp. 433–447, Oct. 2010.

[71] A. Preumont, B. de Marneffe, A. Deraemaeker, and F. Bossens, "The damping of a truss structure with a piezoelectric transducer," *Comput. Struct.*, vol. 86, pp. 227–239, Feb. 2008.

[72] S. S. Aphale, F. A. M. Reza, and S. O. R. Moheimani, "Integral resonant control of collocated smart structures," *Smart Mater. Struct.*, vol. 16, no. 2, pp. 439–446, 2007.

[73] A. Bazaei, Y. K. Yong, S. O. R. Moheimani, and A. Sebastian, "Tracking of triangular references using signal transformation for control of a novel AFM scanner stage," in *IEEE Trans. Control Syst. Technol.*, vol. 20, no. 2, pp. 453–464, Mar. 2012.

[74] I. A. Mahmood and S. O. R. Moheimani, "Making a commercial atomic force microscope more accurate and faster using positive position feedback control," *Rev. Sci. Instrum.*, vol. 80, no. 6, Jun. 2009, Art. no. 063705.

[75] S. Necipoglu, S. Cebeci, Y. E. Has, L. Guvenc, and C. Basdogan, "Robust repetitive controller for fast AFM imaging," *IEEE Trans. Nanotechnol.*, vol. 10, no. 5, pp. 1074–1082, Sep. 2011.

[76] S. S. Aphale, B. Bhikkaji, and S. R. Moheimani, "Minimizing scanning errors in piezoelectric stack-actuated nanopositioning platforms," *IEEE Trans. Nanotechnol.*, vol. 7, no. 1, pp. 79–90, Jan. 2008.

[77] H. R. Pota, I. R. Petersen, and M. S. Rana, "Creep, hysteresis, and cross-coupling reduction in the high-precision positioning of the piezoelectric scanner stage of an atomic force microscope," *IEEE Trans. Nanotechnol.*, vol. 12, no. 6, pp. 1125–1134, Sep. 2013.

[78] Ł. Ryba, A. Voda, and G. Besançon, "An LQG/LTR approach towards piezoactuator vibration reduction with observer-based hysteresis compensation," *IFAC Proc. Volumes*, vol. 47, no. 3, pp. 5623–5628, 2014.

[79] Y. R. Teo, D. Russell, S. S. Aphale, and A. J. Fleming, "Optimal integral force feedback and structured PI tracking control: Application for objective lens positioner," *Mechatronics*, vol. 24, no. 6, pp. 701–711, 2014.

[80] S. K. Das, H. R. Pota, and I. R. Petersen, "Passive damping controller design for nanopositioners," in *Proc. IEEE Amer. Control Conf.*, Jun. 2014, pp. 3645–3650.

[81] N. Kodera, M. Sakashita, and T. Ando, "Dynamic proportional-integral-differential controller for high-speed atomic force microscopy," *Rev. Sci. Instrum.*, vol. 77, no. 8, 2006, Art. no. 083704.

[82] M. S. Rana, H. R. Pota, I. R. Petersen, and H. Habibullah, "Effect of improved tracking for atomic force microscope on piezo nonlinear behavior," *Asian J. Control*, vol. 17, no. 3, pp. 747–761, 2015.

[83] M. Kara-Mohamed, W. P. Heath, Jr., and A. Lanzon, "Enhanced tracking for nanopositioning systems using feedforward/feedback multivariable control design," *IEEE Trans. Control Syst. Technol.*, vol. 23, no. 3, pp. 1003–1013, May 2015.

[84] B. Bhikkaji and S. O. R. Moheimani, "Integral resonant control of a piezoelectric tube actuator for fast nanoscale positioning," *IEEE/ASME Trans. Mechatronics*, vol. 13, no. 5, pp. 530–537, Oct. 2008.

[85] S. K. Das, H. R. Pota, and I. R. Petersen, "Damping controller design for nanopositioners: A mixed passivity, negative-imaginary, and small-gain approach," *IEEE/ASME Trans. Mechatronics*, vol. 20, no. 1, pp. 416–426, Jul. 2015.

[86] S. K. Das, H. R. Pota, and I. R. Petersen, "Resonant control of atomic force microscope scanner: A 'mixed' negative-imaginary and small-gain approach," in *Proc. IEEE Amer. Control Conf.*, Jun. 2013, pp. 5476–5481.

[87] S. K. Das, H. R. Pota, and I. R. Petersen, "Resonant controller design for a piezoelectric tube scanner: A mixed negative-imaginary and small-gain approach," *IEEE Trans. Control Syst. Technol.*, vol. 22, no. 5, pp. 1899–1906, Sep. 2014.

[88] S. K. Das, H. R. Pota, and I. R. Petersen, "Resonant controller for fast atomic force microscopy," in *Proc. IEEE 51st IEEE Conf. Decis. Control (CDC)*, Dec. 2012, pp. 2471–2476.

[89] K. K. Leang and S. Devasia, "Feedback-linearized inverse feedforward for creep, hysteresis, and vibration compensation in AFM piezoactuators," *IEEE Trans. Control Syst. Technol.*, vol. 15, no. 5, pp. 927–935, Aug. 2007.

[90] S. Devasia, "Should model-based inverse inputs be used as feedforward under plant uncertainty?" *IEEE Trans. Autom. Control*, vol. 47, no. 11, pp. 1865–1871, Nov. 2002.

[91] S. Salapaka, A. Sebastian, J. P. Cleveland, and M. V. Salapaka, "High bandwidth nano-positioner: A robust control approach," *Rev. Sci. Instrum.*, vol. 73, no. 9, pp. 3232–3241, 2002.

[92] G. Schitter, P. Menold, H. F. Knapp, F. Allgöwer, and A. Stemmer, "High performance feedback for fast scanning atomic force microscopes," *Rev. Sci. Instrum.*, vol. 72, no. 8, pp. 3320–3327, 2001.
[93] D. Russell, A. J. Fleming, and S. S. Aphale, "Simultaneous optimization of damping and tracking controller parameters via selective pole placement for enhanced positioning bandwidth of nanopositioners," in *Proc. Amer. Control Conf.*, Jun. 2014, pp. 2184–2189.
[94] A. J. Fleming, S. S. Aphale, and S. O. R. Moheimani, "A new method for robust damping and tracking control of scanning probe microscope positioning stages," *IEEE Trans. Nanotechnol.*, vol. 9, no. 4, pp. 438–448, Jul. 2010.
[95] B. Bhikkaji, Y. K. Yong, I. A. Mahmood, and S. O. R. Moheimani, "Diagonal control design for atomic force microscope piezoelectric tube nanopositioners," *Rev. Sci. Instrum.*, vol. 84, Feb. 2013, Art. no. 023705.
[96] S. Hara, Y. Yamamoto, T. Omata, and M. Nakano, "Repetitive control system: A new type servo system for periodic exogenous signals," *IEEE Trans. Autom. Control*, vol. 33, no. 7, pp. 659–668, Jul. 1988.
[97] M. Fairbairn and S. O. R. Moheimani, "Resonant control of an atomic force microscope micro-cantilever for active Q control," *Rev. Sci. Instrum.*, vol. 83, no. 8, 2012, Art. no. 083708.
[98] A. Kotsopoulos, A. Pantazi, A. Sebastian, and T. Antonakopoulos, "High-speed spiral nanopositioning," *IFAC Proc. Volumes*, vol. 44, no. 1, pp. 2018–2023, 2011.
[99] H. Habibullah, H. R. Pota, and I. R. Petersen, "High-precision spiral positioning control of a piezoelectric tube scanner used in an atomic force microscope," in *Proc. Amer. Control Conf.*, Jun. 2014, pp. 1625–1630.
[100] A. Bazaei, Y. K. Yong, and S. O. R. Moheimani, "Combining spiral scanning and internal model control for sequential AFM imaging at video rate," *IEEE/ASME Trans. Mechatronics*, vol. 22, no. 1, pp. 371–380, Feb. 2017.
[101] M. Rafikov and J. M. Balthazar, "On control and synchronization in chaotic and hyperchaotic systems via linear feedback control," *Commun. Nonlinear Sci. Numer. Simul.*, vol. 13, no. 7, pp. 1246–1255, 2008.
[102] A. M. Shawky, A. W. Ordys, L. Petropoulakis, and M. J. Grimble, "Position control of flexible manipulator using non-linear H_∞ with state-dependent Riccati equation," *Proc. Inst. Mech. Eng. I, J. Syst. Control Eng.*, vol. 221, no. 3, pp. 475–486, 2007.
[103] M. J. Balas, "Direct velocity feedback control of large space structures," *J. Guid., Control, Dyn.*, vol. 2, no. 3, pp. 252–253, Jun. 1979.
[104] T. Ando, N. Kodera, Y. Naito, T. Kinoshita, K. Furuta, and Y. Y. Toyoshima, "A high-speed atomic force microscope for studying biological macromolecules in action," *ChemPhysChem*, vol. 4, no. 11, pp. 1196–1202, 2003.
[105] M. Wieczorowski, "Spiral sampling as a fast way of data acquisition in surface topography," *Int. J. Mach. Tools Manuf.*, vol. 41, nos. 13–14, pp. 2017–2022, 2001.
[106] J.-W. Wu, Y.-T. Lo, W.-C. Liu, and L.-C. Fu, "Lissajous scan trajectory with internal model principle controller for fast AFM image scanning," in *Proc. 54th Annu. Conf. Soc. Instrum. Control Eng. Jpn. (SICE)*, Jul. 2015, pp. 469–474.
[107] W. Cai and N. Yao, "Surface modifications with Lissajous trajectories using atomic force microscopy," *Appl. Phys. Lett.*, vol. 107, no. 11, 2015, Art. no. 113102.
[108] E. Csencsics, R. Saathof, and G. Schitter, "Design of a dual-tone controller for lissajous-based scanning of fast steering mirrors," in *Proc. Amer. Control Conf. (ACC)*, Jul. 2016, pp. 461–466.
[109] E. Csencsics and G. Schitter, "Design of a phase-locked-loop-based control scheme for Lissajous-trajectory scanning of fast steering mirrors," in *Proc. Amer. Control Conf. (ACC)*, May 2017, pp. 1568–1573.
[110] M. G. Ruppert, M. Maroufi, A. Bazaei, and S. O. R. Moheimani, "Kalman filter enabled high-speed control of a MEMS nanopositioner," *IFAC-PapersOnLine*, vol. 50, no. 1, pp. 15554–15560, Jul. 2017.
[111] M. S. Rana, H. R. Pota, and I. R. Petersen, "Spiral scanning with improved control for faster imaging of AFM," *IEEE Trans. Nanotechnol.*, vol. 13, no. 3, pp. 541–550, May 2014.
[112] G. E. Fantner, G. Schitter, J. H. Kindt, T. Ivanov, K. Ivanova, R. Patel, N. Holten-Andersen, J. Adams, P. J. Thurner, I. W. Rangelow, and P. K. Hansma, "Components for high speed atomic force microscopy," *Ultramicroscopy*, vol. 106, no. 8, pp. 881–887, 2006.
[113] T. Ando, T. Uchihashi, and T. Fukuma, "High-speed atomic force microscopy for nano-visualization of dynamic biomolecular processes," *Prog. Surf. Sci.*, vol. 83, nos. 7–9, pp. 337–437, 2008.
[114] D. Abramovitch, "Phase-locked loops: A control centric tutorial," in *Proc. Amer. Control Conf. (ACC)*, vol. 1, May 2002, pp. 1–15.

SAJAL K. DAS received the Ph.D. degree in electrical engineering from the University of New South Wales, Australia, in 2014. In May 2014, he was appointed as a Research Engineer at the National University of Singapore (NUS), Singapore. In January 2015, he joined the Department of Electrical and Electronic Engineering, AIUB, as an Assistant Professor. He continued his work at AIUB until he joined the Department of Mechatronics Engineering, Rajshahi University of Engineering & Technology (RUET), as a Lecturer, in September 2015. He is currently an Assistant Professor with RUET. His research interests include control theory and applications, mechatronics system control, robotics, and power system control.

FAISAL R. BADAL was born in Bangladesh. He received the B.Sc. degree in mechatronics engineering from the Rajshahi University of Engineering & Technology (RUET), Rajshahi, Bangladesh. His research interests include control theory and applications, and power system control.

MD. ATIKUR RAHMAN was born in Bangladesh. He is currently pursuing the bachelor's degree in mechatronics engineering with the Rajshahi University of Engineering & Technology (RUET), Rajshahi, Bangladesh. His research interests include control theory and applications.

MD. ATIKUL ISLAM was born in Bangladesh. He is currently pursuing the bachelor's degree in mechatronics engineering with the Rajshahi University of Engineering & Technology (RUET), Rajshahi, Bangladesh. His research interests include control theory and applications.

SUBRATA K. SARKER was born in Bangladesh, in 1996. He received the B.Sc. degree in mechatronics engineering from the Rajshahi University of Engineering & Technology (RUET), Rajshahi, Bangladesh. His research interests include control theory and applications, robust control of electro-mechanical systems, robotics, mechatronics systems, and power system control.

NOROTTOM PAUL graduated from the Rajshahi University of Engineering & Technology (RUET). He is currently pursuing the M.Sc. degree with the Bangladesh University of Engineering & Technology (BUET), with a focus on technology management. He is also an Engineer with the Information and Communication Division, Bangladesh Hi-Tech Park Authority (BHTPA), Bangladesh.